Characterizing and Modeling Wood and Smart Cement with Additives for Real Time Moisture Detection

by
Shivam Bhatia

A thesis submitted to the Civil Engineering Department,
Cullen College of Engineering
in partial fulfillment of the requirements for the degree of

Master of Science

in Civil Engineering

Chair of Committee: Dr. Cumaraswamy Vipulanandan

Committee Member: Dr. Yi-Lung Mo

Committee Member: Dr. Gino J. Lim

University of Houston
August 2020

ACKNOWLEDGEMENTS

This study would not have been possible without valuable assistances of several individuals throughout my research. First, I would like to express my sincere gratitude to my advisor, Dr. C. Vipulanandan, for his valuable guidance, encouragement and kindness throughout my study. I would like to extend my appreciation to Dr. Yi-Lung Mo, Dr. Gino J Lim for serving in my dissertation committee and taking time for exchanging valuable suggestions.

I also want to express my gratitude to my Graduate Advisor, Mr. Jose Rodriguez and to The Director of Graduate Student Affairs, Miranda Vernon-Harrison for their constant guidance throughout my master's program

Special thanks to my family for their encouragement and sacrifice throughout my master's program. I also wish to acknowledge my friends in the GEM group for their help and companionship throughout my research.

The financial support provided by the CIGMAT and THC-IT at the University of Houston is gratefully acknowledged.

ABSTRACT

In this study electrically characterizing the changes in wood (organic) and smart cement (inorganic) due to moisture changes was investigated using 2-probe method. Also, Ultrasonic Pulse Velocity was used to investigate the changes in the compressive wave speed with changes in moisture content.

Smart cement was modified by adding UH-biosurfactant and characterized the changes in the initial resistivity, curing characteristics and the piezoresistive behavior. Also, smart cement was exposed to different water levels (external) and changes in the resistivity were correlated with moisture content. The experimental results were correlated with Vicat Appartus tests and were modeled using Vipulanandan models and Artificial Neural Network (ANN) models.

Wood, one of the most commonly used natural materials was studied for variable moisture saturation conditions and electrical measurements were then recorded to monitor and characterize the changes. Also, Ultrasonic Pulse Velocity test, one of the most established and widely used non-destructive test (NDT) was used to correlate with the moisture changes and resistivity in the wood.

TABLE OF CONTENTS

LIST OF TABLES

LIST OF FIGURES

CHAPTER 1 INTRODUCTION

1.1 General

Cement composites are the most durable construction materials, which are mainly composed of cement, aggregates, water, polymers and different additives (Bastos et al., 2016). The industry of the second most consumed substance in the world behind water is worth over $37 billion, and it employs more than 2 million employees in the United States. It is estimated that around 4.3 million tons of cement were consumed in 2015 worldwide, with a turnover of $335,000 million (Statista, 2017).

Water is a landscape element and a chemically active mobile substance; it is always on continuous move through the surface and subsurface. Frequent handlings of polluting substances on ground surface involve interventions with water quality. Once caught by the moving groundwater, pollutants therefore tend to move along with groundwater, unless chemical reactions influence the mobility of the pollutant (Akankpo and Igboekwe, 2011). With only 3% of the Earth’s water as fresh and 2.5% of the earth's fresh water is unavailable; locked up in glaciers, polar ice caps, atmosphere, and soil; highly polluted; or lies too far under the earth's surface to be extracted at an affordable cost only 0.5% of the earth's water is available fresh water. Added to this is the increasing tendency of building activity along the seaside areas. In seaside areas, the problems of the availability of satisfactory freshwater have led to active consideration of the use of seawater. This practice also cuts down the transportation costs (Thomas and Lisk, 1970).

The cement matrix, which primarily determines the properties of this multi-phase material, consists in a three-dimensional lattice composed of hydrated cement phases (Lea, 2004) and, since the matrix is the continuous phase, it is the one that confers resistance to stresses. The properties of a composite derive both from those of its constituents and form their synergetic interactions (Brandt, 2009).

Mixing conditions including mixing water quality for cement slurries are of great importance. It is not very surprising to see some key cement properties to be impacted by the condition of mixed water. Strength and durability of cement can be reduced due to the presence of chemical impurities in water. Furthermore, cement strength is impacted by the formation of C-S-H (Calcium Silicate Hydrate) gel during cement hydration. Changes in the water chemistry can impact the whole hydration process (Saleh et al., 2018). Hence, monitoring the behavior of cementitious composite with saline water is critical during the construction and entire service life in order to certify the safety of the composite.

Vipulanandan et al., (2014) developed Chemo-piezo sensitive cement with an improvised electrical method to monitor the cement behavior. Electrical Resistivity of cementitious materials is used as a sensing property to quantify changes due to contaminations for quality control throughout its construction and service life.

Until this century wood was the single greatest material aid and comfort in every century of our ancestors lives. The first everything; including the first submarine and airplane; were first made of wood. Wood was being shaped into homes: windbreaks were erected before the entrances of caves, cooking and eating utensils were fashioned. The importance of wood in the lives of our ancestors is outweighed by no other single material. Wood is the most important material contact we have with the entire body of our ancestry. It has been paramount in aiding, comforting and paving the road to civilization (Kramer, 2006). Wood is still essential to human life, but it has evolved over the ages from a simple, readily available material to a modern industrial and engineering material (Youngs). Our present use of wood is restricted to fast growth softwoods and a few hardwoods for trim and decoration. The cost of wood is steadily rising, and supplies are growing smaller. If we survive the lack of air a lack of trees will provide; there will still be no wood for new work; the age of wood will have finally passed from the epoch of

civilization. What little then remains will be the very last (Kramer, 2006). It is critical for us to use our wood resources efficiently.

Along with deforestation, wood decay and degradation are the primary reasons for the limited supplies of wood. Hence there is a need to detect the changes occurring in the wood due to external factors such as moistures; as they are primarily responsible for wood degradation.

Nondestructive measurements such as electrical measurements and ultrasonic pulse velocity are used to detect the changes in the wood configuration due to changes in the moisture content.

1.2 Problem Statement

One of the major probelm in the construction indutry is real time monitoring of cementitious composites, starting from its construction throughout its service life. This could very well be answered by the application of Smart Cement; a chemo-piezo sensitive material. But there is an emergnig challenge to verify the applicability of smart cement due to various modifications. Characterizing the smart cement material sensitive to contaminations, stresses, variable external conditions such as mositure infiltration; helps us to widen the appliaction of smart cement. Hence it is necessary to perform a systematic characterization of smart cement composites to monitor the changes in the material during its hydration.

There is a growing worry about the increasing demand of wood along with its scarcity due to wood decay and degradation. Moisture attack is one of the primary reasons of wood decay. Hence it is important to characterize the wooden configuration through various moisture changes.

1.3 Objectives

The overall objective was to develop and characterize smart cement and wood using the electrical measurements under application of variable moisture conditions. The specific objectives are as follows:

1. Characterize the Curing and Piezoresistive behavior of Smart Cement composite with additives under the effect of stress and variable moisture conditions.
2. Characterize the configuration of wood along with its changes in moisture content

1.4 Organization

This study is organized into five main chapters. Chapter 1 is the introduction of this research, which leads to a problem statement and the detailed objective of this study. Chapter 2 provides the literature review related to smart cement, electrical measurement techniques for cementitios materials and wood, bosurfactants and the artificial neural network. Chapter 3 discusses the materials used for the preparation of smart cement composites and the experimental techniques followed in this study. Chapter 4 provides the complete characterization of smart cement. It discusses the test results of additive modification on the resistive and piezoresistive properties of smart cement composites. Experimental results have been modelled using Vipulanandan and ANN models. Chapter 5 specifies the alterations tree cover across United States. Also, results of the nondestructive testing with moisture changes in wood have been discussed. Finally, the conclusions of this research and recommendations for further work have been summarized in chapter 6.

CHAPTER 2 BACKGROUND AND LITERATURE REVIEW

2.1 Introduction

This chapter provides a brief description on the related topics to the field of study. It summarizes the literature review conducted on methods for measuring the electrical resistivity, hydration monitoring techniques for cement and electrical methods to monitor the health of wood

2.2 Smart Cement

Monitoring of structures by embedded or attached sensors has been gaining increasing interest and is more effective to guarantee the structural safety in service. However, smart cement which can sense its own damage is more attractive due to its strong mechanical properties and self-monitoring characteristics. Smart cement with conductive filler has been systematically developed (Vipulanandan, et al. 2004-2013). In this technology, cement itself is a sensor. Therefore, there is no need to embed strain gauges, optical fibers or other sensors in the cement.

Advantages of Smart Cement:

1. Facilitates the real time monitoring of cementitious materials during and after construction.
2. Monitors stresses in the cement and notifies about the risk of possible damage to provide the opportunity for repair and reconstruction.
3. Advises about the extent of setting time of cement; thereby allowing safe construction process.
4. Monitors the quality of cement using electrical resistivity measurements.

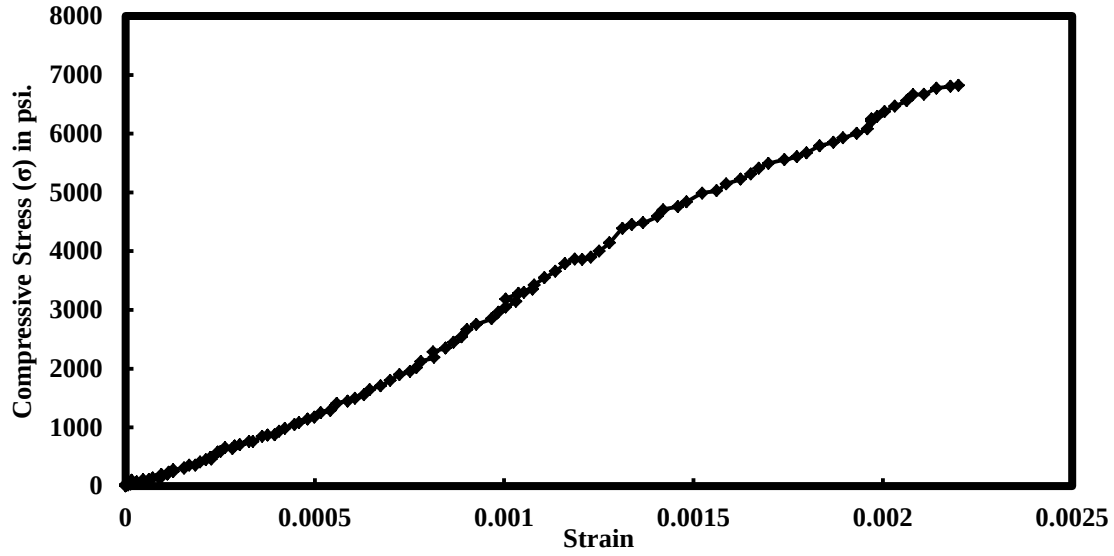

Figure – 2.1 Typical Stress Strain Behavior of Cement Composite
(Data from Praveen, 2014)

The smart cement technology can monitor the changes in the cement at very high magnification of about 2500 times after one day curing. The main property of interest is piezoresistivity, the change in the resistivity of the cement with the application of the stress. (Vipulanandan et al., 2014).

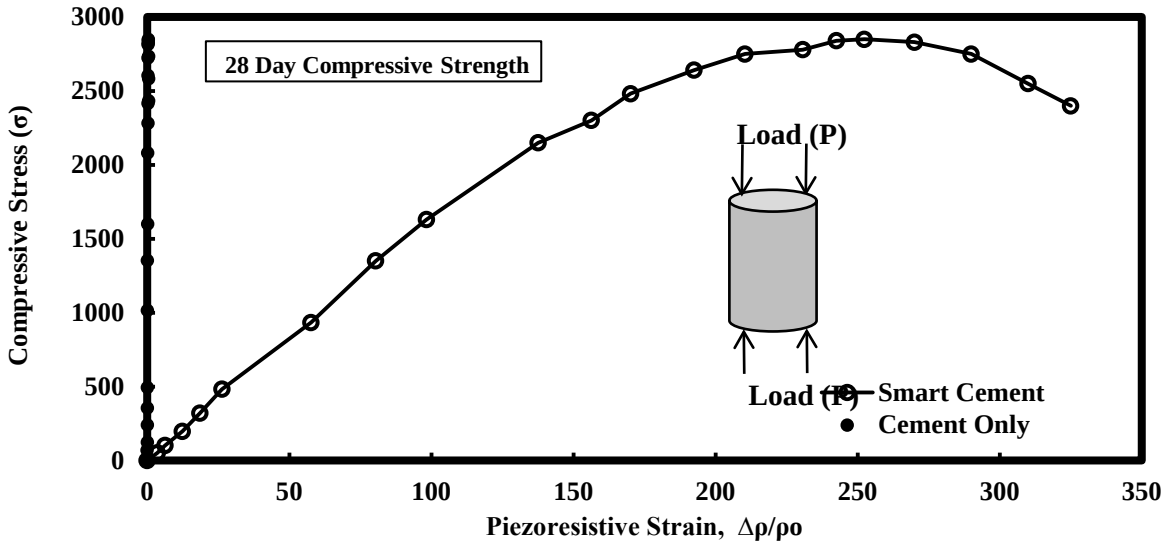

Figure – 2.2 Typical Piezoresistive behavior of cement composite
(Data from: Vipulanandan et al., 2014)

The work of many researchers on the electrical resistance and resistivity applications for cementitious materials has been investigated in detail.

Table 2-1:Summary of Electrical Characterization of Cementitious Materials

Reference	Materials	Water Cement Ratio	Fibers Used	Measurement Techniques	Parameters Studied	Remarks
Banthia, et al. (1992)	Silica Fume / Cement = 0.2	0.3	Carbon fibers and steel fibers (5% by volume)	AC, 2 probe, copper electrode	Resistance, Electrical Resistivity	Effect of fiber type, inter-electrode spacing and age of specimen on Electrical Resistivity
Han, et al. (2009)	Portland Cement	N/A	Carbon nanotube (0.1% by wt. of cement)	2 probe method	Resistance, Change in Resistance, Vehicle speed	1) Response of electrical resistance to compressive loading 2) Self-sensing CNT composite has a potential for traffic monitoring
Han, et al. (2009)	Portland Cement, silica fume (15% by wt. of cement)	N/A	Nickel Powder	DC 4 probe method, 1.5 V	Electrical Resistivity, Compressive stress, Compressive strain	Relationship between Change in Electrical Resistivity and Compressive stress and Compressive strain
Topcu, et al (2011)	Ordinary Portland Cement, Fly-ash, silica fume, blast furnace slag	0.4-0.55	N/A	AC, 2 robe, copper plate	Setting time, Electrical conductivity. Compressive strength	(1). Relationship between conductivity and time. (2) Effect of additives on conductivity.

Table 2-1:Summary of Electrical Characterization of Cementitious Materials (continued)

Reference	Materials	Water Cement Ratio	Fibers Used	Measurement Techniques	Parameters Studied	Remarks
Xiao, et al. (2011)	Portland Cement (Type I)	0.3 – 055	N/A	Non-contact Electrical Resistivity measurement	Electrical Resistivity (ER), Compressive strength	1) Relation between ER and W/C 2) Correlation between compressive strength and ER.
Spragg, et al. (2013)	Portland Cement (Type I)	0.42	N/A	2 probe (plate electrodes and embedded electrode rods), 4 probe method	Specimen Geometry, specimen temperature, sample storage, Electrical Resistivity	1) Influence of specimen geometry, temperature and storage condition on resistivity. 2) Impedance response for different specimen geometry with frequency.
Hambach, et al. (2015)	Portland cement	0.35	Carbon fiber (1% - 4% by volume)	2 Probe Method	Flexural strength, Electrical heating test	Applicability of in-situ heating of carbon fiber based cement based flooring
Sun, et al. (2015)	Portland cement	0.41 – 0.55	Carbon fiber mat (0% - 1.2% by volume)	4 probe method	Resistivity, Compressive strength	1) Variation in resistivity with curing period and carbon fiber content 2) Effect of carbon fiber content on compressive strength

Table 2-1:Summary of Electrical Characterization of Cementitious Materials (continued)

Reference	Materials	Water Cement Ratio	Fibers Used	Measurement Techniques	Parameters Studied	Remarks
Wang, et al. (2016)	Portland cement (TypeI), superplasticizer (0% - 0.8% by solid wt.)	0.3	N/A	Non-contact Electrical Resistivity Apparatus	Electrical Resistivity Setting time, Compressive strength, Heat evolution.	1) Variation in Electrical Resistivity with time. 2) Rate of heat evolution with time
Tiexeria, et al. (2015)	Portland cement (Type 1)	0.5	TiO2 (0.8% - 5% by wt. of cement)	DC, 2 Probe metal electrodes	Electrical Resistivity (ER), Compressive strength, Porosity	1) AC – 2 probe method. 2) Electrical Resistivity, fiber content, Compressive stress.
Remarks	Portland cement	0.3 – 0.55	Carbon fibers	AC – 2 probe	Electrical Resistivity, Compressive strength	1) AC-2probe method. 2) Electrical Resistivity, fiber content, Compressive stress

2.3 Wood

Significant efforts have been made to develop robust, non-destructive technologies (NDT) capable of predicting the intrinsic wood properties of individual living trees and assessing wood quality by stand and forest. In addition, non-destructive technologies including (mini) rhizotrons and ground-penetrating radar have been recently proposed to assess plant rooting distribution and growth (Sanesi et al. 2013, Marziliano et al. 2015). The use of such technologies not only leads to greater profitability for the forest industry but can also help foresters to make economic and environmental management decisions for treatment of individual trees and forest stands, improve thinning and harvesting operations, and efficiently allocate timber resources for optimal utilization (Wang et al. 2007a, Proto et al. 2014).

Acoustic technologies have become well established as material evaluation tools, and their use has become widely accepted for quality control by the wood industry (Wang et al. 2007b). With the development of portable and simple-to-use, time-of-flight and resonance-based tools, the use of acoustics in the forestry sector has increased, particularly in countries such as New Zealand (Walker & Nakada 1999, Tseheye et al. 2000, Chauhan & Walker 2006), Australia, USA (Wang et al. 2001, 2004), Hungary (Brashaw et al. 2009, Divos 2010) and the United Kingdom (Searles & Moore 2009).

Researchers have also started to consider detection based on electrical resistivity of wood owing to the advantages offered by this method in detecting the quality or service life as an indicator of fluid transport properties of the sample. Wood is an extremely complex organic matter with the characteristics of porosity, hygroscopicity and anisotropy. Hence electrical resistance is affected by the moisture content in the sample, temperature of the sample, direction of the flow of current (parallel or perpendicular to fibers), species and density of wood and extent of specimen beyond the electrode.

Following table demonstrates the literature review on the Non-Destructive Testing conducted on wood.

Table – 2.2 Summary of Electrical Measurement Techniques for Wood

REFERENCE	APPARATUS	FREQUENCY	PARAMETERS EVALUATED	MODEL EQUATION	CONCLUSION	REMARKS
Stamm (1927)	Megger Insulation tester	N/A	Electrical Resistance (ER), Moisture content, Density, Direction of flow of current, temperature		ER changes with moisture content but within narrow limits.	ER is largely affected by the directions of wooden wood grains
Kumar, et al. (1993)	Digital Multimeter	N/A	Electrical Resistivity, carbonization temperature		Resistivity decreased with increase in carbonization temperature	Cellulose and Legnin affect the ER. Acia is higher in cellulose than Eucalyptus
Sahin, et al. (2004)	Standing wave ratio meter	9.8GHz and 2.45GHz	Dielectric properties, directional properties		dielectric properties increase with rising moisture content	Dielectric constant of water is about 2500 times higher than wood, so there's increase in dielectric constant of wood
Hasenstab, et al. (2006)	A flash tube XR200	Longitudnal wave - 100kHz Transverse wave – 55kHz	Time of flight		Ultrasound technique is sensitive to cracks parallel to surface and X-Ray technique for perpendicular to surface.	Longitudinal waves are more sensible to cracks than transverse waves

Table – 2.2 Summary of Electrical Measurement Techniques for Wood (continued)

REFERENCE	APPARATUS	FREQUENCY	PARAMETERS EVALUATED	MODEL EQUATION	CONCLUSION	REMARKS
Husein, et al. (2014)	3532-50 LCR HiTESTER (Hioki)	10, 100, 10^3, 10^4, 2 x10^4, 4 x 10^4, 6 x 10^4, 8 x 10^4 and 10^5 Hz	Electrical conductivity, Impedance, directional property		Semiconductor when conductivity is in the range of 10^{-3} to 10^3 S/cm (10^3 – 0.001 Ωm)	Effect of wood species on ER is marked upto the carbonization temperature of 800 °C
Yue, et al. (2018)	The PICUS Tree Tronic Tree Electrical Resistance Tomography	N/A	Electrical resistance, moisture content, temperature.	**Sound trees:** Log R = -0.5(T) - 0.02(MC) +6.34 **Decayed trees:** LogR = -0.44(T) -0.01 (MC) +5.93	Application of ERT can separate sound and decay trees	ER is largely affected by temperature hence there is a need to calibrate the effect of temperature
Yue, et al. (2019)	PICUS Tree Tronic Electrical Resistance Tomography and Arbotom Stress Wave Tomography	N/A	Electrical resistance, degree of decay by ERT(De), degree of decay by SWT (Ds), mass loss of sample due to decay (Dt)	De = 0.6659 Dt +11.852, Ds = 0.9993 Dt +7.5369	Electric resistance tomography showed better results than stress wave tomography	Correlations can be made between the severity of decay and detected by ERT and true severity of decay
REMARKS	Nondestructive methods	10^4 for measuring ER	Electrical Impedance, Electrical Resistivity.	Equations used for correlation needs accuracy.	Electrical properties very sensitive to wood configuration	Ability to detect changes in the wood composition

Table – 2.3 Electrical Resistivity of different materials

Material	**Resistivity, ρ (Ω.m)** at 20 °C
Silver	1.59×10^{-8}
Copper	1.68×10^{-8}
Gold	2.44×10^{-8}
Aluminum	2.82×10^{-8}
Calcium	3.36×10^{-8}
Tungsten	5.60×10^{-8}
Zinc	5.90×10^{-8}
Nickel	6.99×10^{-8}
Lithium	9.28×10^{-8}
Iron	1.0×10^{-7}
Platinum	1.06×10^{-7}
Tin	1.09×10^{-7}
Carbon steel	10^{10}
Lead	2.2×10^{-7}
Titanium	4.20×10^{-7}
Stainless steel	6.9×10^{-7}
Mercury	9.8×10^{-7}

Table – 2.3 Electrical Resistivity of different materials (continued)

Carbon (diamond)	1×10^{12}
Sea water	2×10^{-1}
Drinking water	2×10^{1} to 2×10^{3}
Silicon	6.40×10^{2}
Deionized water	1.8×10^{5}
Glass	10×10^{10} to 10×10^{14}
Hard rubber	1×10^{13}
Wood (oven dry)	1×10^{14} to10^{16}
Sulfur	1×10^{15}
Air	1.3×10^{16} to 3.3×10^{16}
Paraffin wax	1×10^{17}
Fused quartz	7.5×10^{17}
PET	10×10^{20}
Teflon	10×10^{22} to 10×10^{24}

2.4 Bio-Surfactants

Biosurfactant usually refers to surfactants of microbial origin (Mulligan, 2005). They are expected to become known as multifunctional materials of the twenty first century as they have applications in different industrial processes as well as potential novel future uses (Marchant and Banat, 2012) mostly due to their diverse structures. The composition and yield of biosurfactants

depends on bioreactor characteristics, pH of the medium, nutrient composition, agitation, oxygen availability, and temperature (Costa et al., 2018)

The biosurfactant is produced from waste oil with acclimated bacteria in continuously stirred batch reactor (Harendra et al., 2008; Vipulanandan et al., 2000). It is water soluble.

2.5 Artificial Intelligence

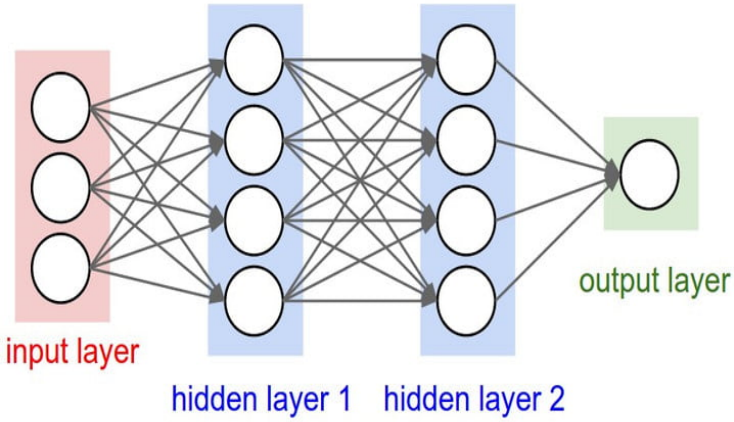

Figure – 2.3 Artificial Intelligence

Artificial Intelligence (AI), otherwise known as machine learning or computational intelligence, is the science and engineering aimed at creating intelligent tools, devices and machines. Its application in solving complex problems and case-based complications in various field applications has become more and more popular and acceptable over time (Opeyemi et al., 2016).

2.5.1 Artificial Neural Networks

An artificial neural network (ANN) is a computational numerical model which is based on, at some level, brain like learning as opposed to traditional computing which is based on programming. Artificial neural networks are one of the main tools used in machine learning. As the “neural” part of their name suggests, they are brain-inspired systems which are intended to replicate the way that we humans learn. Neural networks consist of input and output layers, as well as (in most cases) a hidden layer consisting of units that transform the input into something

that the output layer can use. They are excellent tools for finding patterns which are far too complex or numerous for a human programmer to extract and teach the machine to recognize (Dormehl, 2019). While neural networks (also called “perceptrons”) have been around since the 1940s, it is only in the last several decades where they have become a major part of artificial intelligence. Warren S. McCulloch and Walter H. Pitt’s 1943 paper, ‘‘A Logical Calculus of the Ideas Immanent in Nervous Activity,’’ is often cited as the starting point in neural network research.

The artificial neural network is a numerical model. It consists of many artificial neurons interconnected where each of them gives a single output (Y) induced from all inputs (Xi) (Hammoudi et al., 2019). The predictive capability of artificial neural networks comes from the ability to learn and adapt to new situations in which additional data becomes available. The first layer (input layer) consists of neurons representing the independent variables (inputs Xi), the second one is the hidden layer (Hi, f(Hi)), and the last one is the ANN responses (output layer, representing AI). The number of neurons required in the hidden layer is determined in a way to minimize both prediction error and number of neurons. The general forms of the equations are as

$$Hj = \sum WijXi + bj \qquad (2.1)$$

where Xi represent the inputs (Figure 2-4, neurons I) and subscript i represents the inputs (I and summation 1 to n). The Wij is the weighing matrix for each input term Xi connecting it to the hidden term Hj, the bj is the bias input function.

2.5.2 How do neural networks work?

Let us take the example of the price of a property and to start with we have different factors assembled in a single row of data: Area, Bedrooms, and Distance to city and Age.

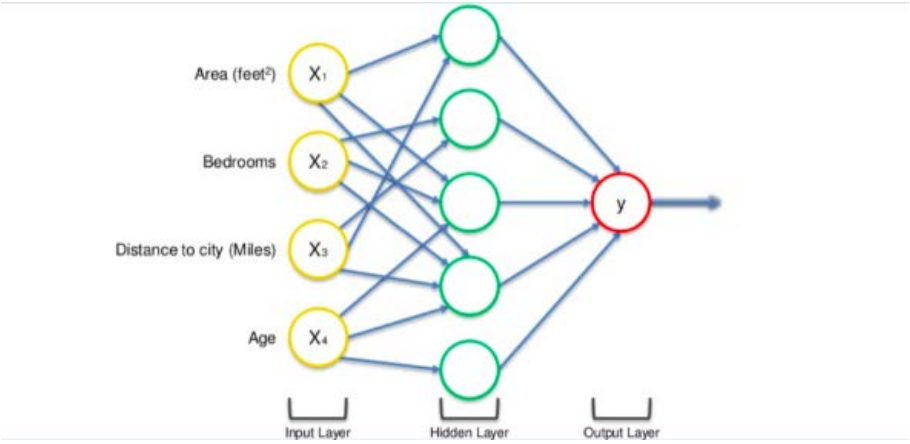

Figure – 2.4 An illustration of a neural network

The input values go through the weighted synapses straight over to the output layer. Now in the above figure, all 4 variables are connected to neurons. They will either have a 0 value or non-0 value.

Here, the non-0 value → indicates the importance and 0 value → they will be discarded.

Let's take the example of Area and Distance to City is non-zero for the first neuron, which means they are weighted and matter to the first neuron. The other two variables, Bedrooms and Age aren't weighted and so are not considered by the first neuron.

You may wonder why that first neuron is only considering two of the four variables. In this case, it is common on the property market that larger homes become cheaper the further they are from the city. That's a basic fact. So what this neuron may be doing is looking specifically for properties that are large but are not so far from the city.

Now, this is where the power of neural networks comes from. There are many of these neurons, each doing similar calculations with different combinations of these variables. Once this criterion has been met, the neuron does its calculations. The next neuron down may have weighted synapses of Distance to the city and, Bedrooms.

This way the neurons work and interact in a very flexible way allowing it to look for specific things and therefore make a comprehensive search for whatever it is trained for.

2.5.3 How do neural networks learn?

Learning in a neural network is closely related to how we learn in our regular lives and activities we perform an action and are either accepted or corrected by a trainer or coach to understand how to get better at a certain task. Similarly, neural networks require a trainer in order to describe what should have been produced as a response to the input. Based on the difference between the actual value and the predicted value, an error value also called **Cost Function** is computed and sent back through the system.

For each layer of the network, the cost function is analyzed and used to adjust the threshold and weights for the next input. Our aim is to minimize the cost function. The lower the cost function, the closer the actual value to the predicted value. In this way, the error keeps becoming marginally lesser in each run as the network learns how to analyze values.

We feed the resulting data back through the entire neural network. The weighted synapses connecting input variables to the neuron are the only thing we have control over.

As long as there exists a disparity between the actual value and the predicted value, we need to adjust those weights. Once we tweak them a little and run the neural network again, a new Cost function will be produced, hopefully, smaller than the last. We need to repeat this process until we scrub the cost function down to as small as possible.

The procedure described above is known as **Back-propagation** and is applied continuously through a network until the error value is kept at a minimum.

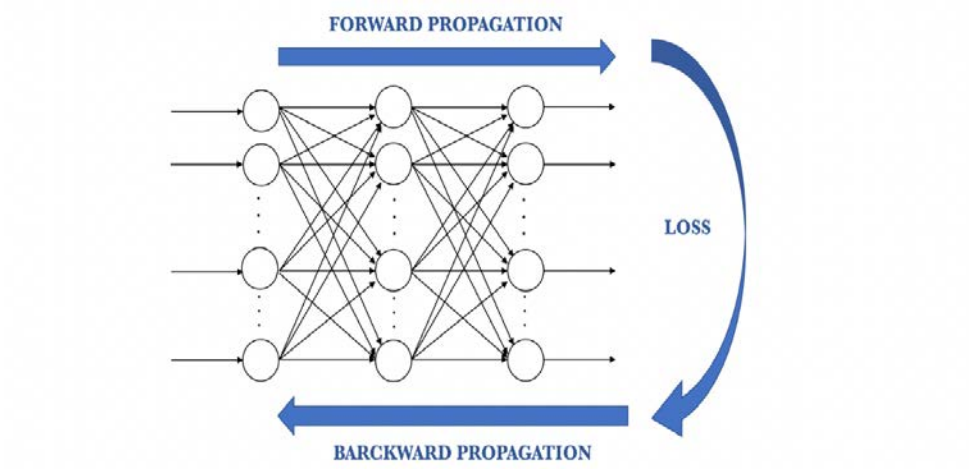

Figure – 2.5 Backward Propagation of Neural Networks

2.6 Summary

Based on the literature review conducted on measurement techniques to monitor cementitious materials and wood, Artificial Intelligence and Bio-surfactants; following can be summarized:

1. Various conductive fillers have been used to enhance the pressure sensing capability of cementitious materials.
2. Use of electrical resistivity as a monitoring tool for monitoring the behavior of cementitious composites is well established. Very few researchers have tried the two probe method using Alternating Current.
3. Neural networks are a new concept whose potential we have just scratched the surface of. By properly minimizing the error, these multi-layered systems may be able to one day learn and conceptualize ideas alone, without human correction.
4. The potential applications of Bio-surfactants include such as herbicides and pesticides formulations in agricultural industry, detergents, healthcare and cosmetics, textiles, ceramic processing and food industries with Oil industry being the largest market.

CHAPTER 3 MATERIALS AND METHODS

Introduction

In this chapter, a brief description of the different types of materials used and the testing methods adopted have been summarized. Materials of interest, equipment used, sample preparation, compression test and electrical resistivity measurements are discussed.

3.1 Materials

3.1.1 Cement

For the entire extent of this study, commercially available Class H type of cement was used.

3.1.2 Smart Cement

Commercially available Class H cement was modified by adding conductive fillers (0.04% by weight of cement) for w/c 0.4, thereby developing a piezoresistive material.

3.1.3 UH – Biosurfactant

The biosurfactant is produced from waste oil with acclimated bacteria in continuously stirred batch reactor (Harendra et al., 2008; Vipulanandan et al., 2000). The biosurfactant is water soluble and based on Fourier Transform Infra Read (FTIR) spectroscopy analyses both carboxyl (COO-) and hydroxide (OH-) groups were identified in the biosurfactant.

3.1.4 Wood

Commercially available softwood used for this study has density in the range of 0.49 to 0.51gm/cm^3.

3.1.5 Water

Tap water has been used for this study. Although, for the some part of this study; commercially available salt has been added to tap water; to form salty water.

3.2 Equipment

LCR Meter

Commercially available Keysight Precision LCR Meter (Figure – 3.1) is used to measure the Resistance (R) of specimens at different frequencies. Measured resistance is then converted to Resistivity (ρ) using the formula ρ = R*(A/L). The frequency range for measuring the resistance is from 20 Hz to 300 kHz.

Conductivity Probe

Commercially available Oakton COND 6+ conductivity probe (Figure – 3.2) was used to measure the resistivity of different samples. The range for measuring conductivity is from 0.1µS/cm to 1000mS/cm. Conductivity meter was first calibrated using standard solution with a known value of conductivity. After calibration, the device was double checked with another standard solution for consistency. The conductivity probe was calibrated using standard solution of sodium chloride (NaCl).

Figure – 3.1 LCR Meter

Figure – 3.2 Conductivity probe

Vernier Caliper

For this study, commercially available Westward Digital Vernier Caliper was used to measure the dimensions of different specimen and samples. The caliper is made of carbon fiber composite and has an accuracy of 0.01”.

Compression Testing Machine

Compression tests were performed on the cylindrical specimen using a Hydraulic compression machine.

3.3 Testing Methods

Electrical Resistivity

After numerous studies by Vipulanandan et al., (2004, 2013 and 2014), electrical resistivity (ρ) was selected as the sensing property for cement-based materials. Resistivity and change in resistivity were used to quantify the sensing properties of the cement.

Electrical Resistivity can be expressed as

$$\rho = \frac{R}{K + GR}. \qquad (3.1)$$

Conductivity meter was used to measure the Resistivity of cement slurry. But measuring the resistivity of hardened cement paste was a challenge due to the limitation of devices. Also, correlating the resistivity with other parameters was impracticable due to the uncertainty in the actual path of current in the specimen. Hence, Electrical Resistance is measured by LCR device throughout its curing duration. Using Resistance and the k-factor (from eq^{n} 1), resistivity can be determined for cement paste in hardened state.

Piezoresistivity

Piezoresistivity describes the change in the electrical resistivity of a material when subjected to stress. In this study hardened cement paste will be tested and characterized. During the compression test, electrical resistance was measured in the direction of the applied stress. To eliminate the polarization effect, AC resistance measurements were made using an LCR meter at frequency of 300 kHz (Vipulanandan et al., 2013).

Shrinkage

Loss of moisture during hydration period is the main reason for shrinkage. Shrinkage studies were conducted on the hardened specimen, using a vernier caliper. To measure shrinkage, change in dimensions was measured (vertically and radially) over the period of curing duration. Volumetric Shrinkage can be calculated by: $\Delta v = [V_{(t)} - V_{(0)}] / V_0$ **(3.2)**

where, $V_{(t)}$ = volume at any time and $V_{(0)}$ = initial volume.

Density

Density of Smart Cement specimen was calculated and monitored throughout the curing duration. Density is a material property and hence can be useful for detecting the changes in specimen due to external factors.

Vicat Apparatus

Setting Time is an important parameter in the quality control. The initial and final setting time is determined by vicat apparatus that has been standardized in ASTM C191-19**.** Vicat apparatus is a device for determining the normal consistency and time of setting of cement that consists of a rod weighing 300 grams, having a needle in each end, and supported in a frame with a graduated scale to measure the distance to which the needle penetrates the cement.

Ultrasonic Pulse Velocity

Ultrasonic Pulse Velocity was used to investigate the changes in the compressive wave speed of wood due to changes in its moisture content. Measurements were conducted using 150 kHz transducers which were kept in complete contact with the wooden specimen.

3.4 Cement Mixing Procedure

Smart Cement prepared with w/c 0.4, is used in this study. Firstly, all the required materials were weighed and collected in separate containers. Conductive fillers were hand mixed in water, part by part, till the fillers were properly dispersed in water and no clusters were formed. Cement, was then gradually added to this and hand-mixed for about 15 minutes, to obtain a

uniform consistency of the slurry (Figure – 3.3). Mixing was done in the laboratory at room temperature of about of 23±2 ℃.

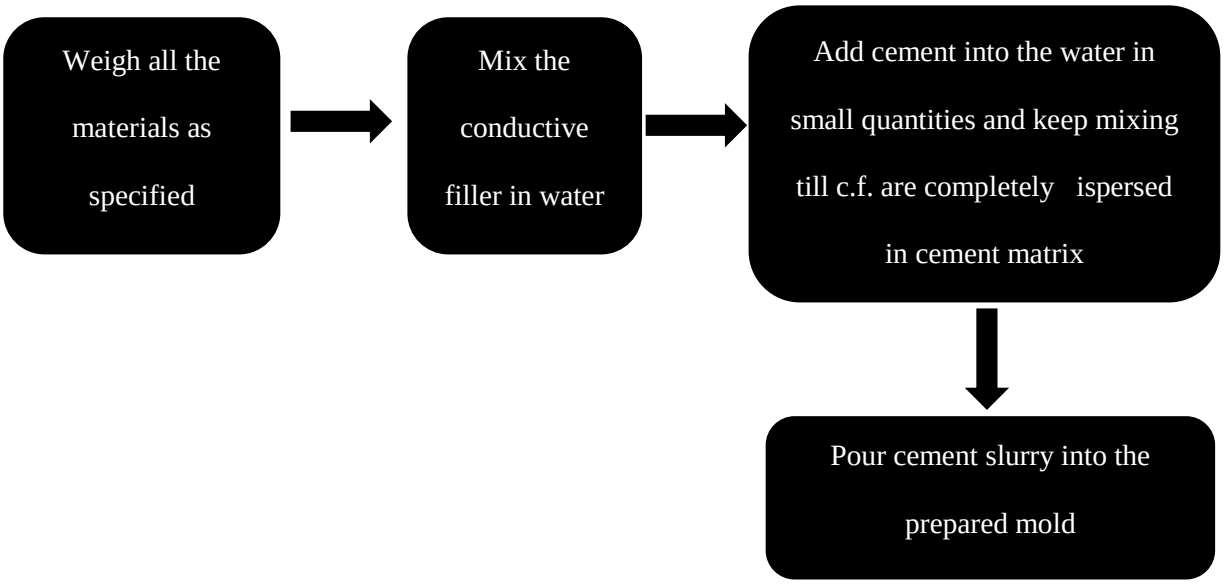

Figure – 3.3 Standard Mixing Method for Smart Cement Samples

The prepared slurry was poured into cylindrical molds of 4” height and 2” diameter. Four conductive wires were placed in the mold for electrical measurements (Figure 3.4). Specimens were demolded after 24 hours. Continuous monitoring of the samples was done for 28 days.

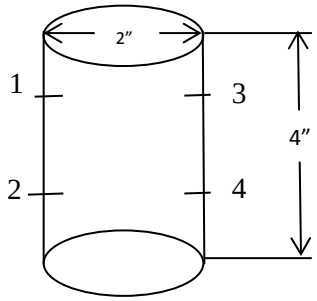

Figure – 3.4 Cylindrical mold for Smart Cement Specimen

In the tests where saline water was used to prepare smart cement specimen, required amount of salt was first added to water and then conductive fillers was added, followed by the standard mixing method of smart cement specimen.

3.5 Modelling

Modelling is important as it is a simplified representation that enables predictions to be developed and tested by experiments. In this section, different models used in this study have been discussed.

3.5.1 Impedance Model

In this study, different electrical circuits are studied to find an appropriate curcuit to represent the behavior of the material under study.

Case 1: General Bulk Material – Capacitance and Resistance

Case 1 explains about the general bulk materials that involves resistor and capacitor

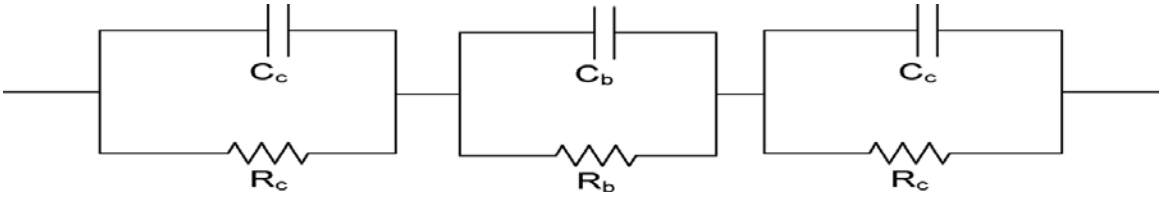

Figure – 3.5 Equivalent Circuit for Case 1

Here contacts are connected in series whereas the contacts and bulk material are connected in parallel using a capacitor and resistor. Both contacts are represented by same resistance (R_c) and capacitance (C_c) because they are identical. R_b and C_b are the resistance and capacitance of the bulk material respectively, and R_c and C_c are the resistance and capacitance of the contacts, respectively.

The total impedance of the equivalent circuit for case 1 (Z_1) at any applied stress (σ) can be represented as follows: [Vipulanandan and Prashanth (2013)]

$$Z_1 = \frac{R_b}{1 + \omega^2 R_b^2 C_b^2} + \frac{2 R_c}{1 + \omega^2 Rc^2 Cc^2} - j \left\{ \frac{2\omega Rc^2 Cc}{1 + \omega^2 Rc^2 Cc^2} + \frac{\omega R_b^2 C_b}{1 + \omega^2 R_b^2 C_b^2} \right\} \quad \textbf{(3.3)}$$

when the frequency of the applied signal is very low, $\omega \rightarrow 0$, $Z_1 = R_b + 2R_c$, and when it is very high, $\omega \rightarrow \infty$, $Z_1 = 0$ (See Figure 3.7).

Case 2: Special Bulk Material - Resistance Only

Case 2 is a special case of case 1. It explains about special bulk material represented by a resistor (R_b) whereas the capacitance of the bulk material (C_b) is assumed to be negligible. Contacts (wires) are represented by resistor (Rc) and capacitor (Cc) in parallel. Contacts are connected to bulk in series.

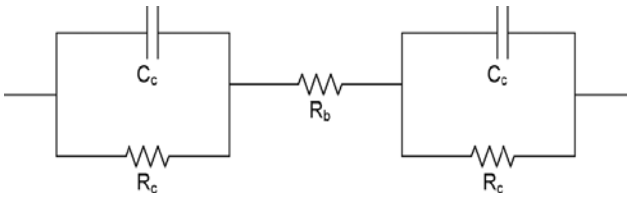

Figure – 3.6 Equivalent Circuit for Case 2

The total impedance of the equivalent circuit for case 2 (Z_2) can be represented as follows: [Vipulanandan and Prashanth (2013)]

(3.4)

$$Z_2 = R_b + \frac{2R_c}{1+\omega^2 Rc^2Cc^2} - j\frac{2\omega Rc^2Cc}{1+\omega^2 Rc^2Cc^2}$$

when frequency of applied signal is low i.e. $f \rightarrow 0$, $\omega = 2\pi f \rightarrow 0$, $Z_2 = R_b + 2R_c$ and when the frequency is very high i.e. $f \rightarrow \infty$, $\omega = 2\pi f \rightarrow \infty$, $Z = Rb$ (See figure figure 3.7)

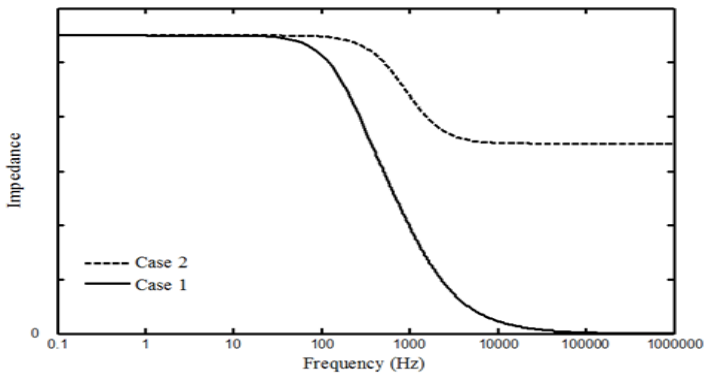

Figure - 3.7 Comparisons of Typical Responses of Equivalent Circuits for Case 1 and Case 2

The shape of the curves shown in figure 3.7 is very much influenced by material response and the two probe instruments used for monitoring. Testing of smart cement indicated that Case 2

represented their behavior and hence the bulk material properties can be represented by resistivity and characterized at a frequency of 300 kHz using the two probes.

3.5.2 Electrical Resistivity Model

To characterize the resistivity of the hardened cement, p-q model (Vipulanandan and Paul, 1990) can be used, which is defined as

$$\frac{1}{\rho(t)} = \left(\frac{1}{\rho_{min}}\right) \frac{\left(\frac{t+t_0}{t_{min}}\right)}{q_1 + (1-p_1-q_1) * \left(\frac{t+t_0}{t_{min}}\right) + p * \left(\frac{t+t_0}{t_{min}}\right)^{\frac{q_1+p_1}{p_1}}} \quad \textbf{(3.5)}$$

where $\rho\ (t)$ is electrical resistivity that changes with the curing time (t), ρ_{min} is the minimum electrical resistivity, t_{min} is time corresponding to minimum electrical resistivity, $p(t)$ and $q(t)$ are time dependent model parameters. ρ_{min}, t_{min} and t_0 are time independent model parameters that will explain the changes occurred due to the addition of the materials to the cement slurry.

3.5.3 Piezoresistivity Model

Piezoresistivity shall be modeled using p-q model (Vipulanandan and Paul, 1990) which can be used as

$$\sigma = \frac{\sigma_{max} \times \left(\frac{\left(\frac{\Delta\rho}{\rho}\right)}{\left(\frac{\Delta\rho}{\rho}\right)_0}\right)}{q_2 + (1-p_2-q_2) \times \left(\frac{\left(\frac{\Delta\rho}{\rho}\right)}{\left(\frac{\Delta\rho}{\rho}\right)_0}\right) + p_2 \times \left(\frac{\left(\frac{\Delta\rho}{\rho}\right)}{\left(\frac{\Delta\rho}{\rho}\right)_0}\right)^{\left(\frac{p_2+q_2}{p_2}\right)}} \quad \textbf{(3.6)}$$

where σ_{max} is the maximum stress at failure, $(\Delta\rho/\rho)_0$ is the piezoresistivity of the hardened cement under the maximum stress, $(\Delta\rho/\rho)$ is the piezoresistivity at any stress σ and p_2 and q_2 are experimentally fit parameters.

3.5.4 Artificial Neural Network Model

ANN is a multilayer perceptron (MLP) including three layers. The first layer (input layer), the second one is the hidden layer, and the last is the ANN response (output layer). The

number of neurons required in the hidden layer is determined in a way to minimize both prediction error and number of neurons.

The following function is used for ANN prediction:

Sigmoid fun $f(x) = 1/(1 + e^{-x})$. **(3.7)**

3.6 Summary

The summary of experimental study is as follows.

1. For measuring the electrical resistance, AC measurements were performed from 20 Hz to 300 kHz using LCR meter and the behavior of material was characterized based on the impendence response.
2. Standard conductivity meter was used to determine the resistivity of different modified cement specimens in slurry state.
3. Tinius Olsen, a hydraulic testing machine was used to test smart cement specimens under compression in room temperature and pressure conditions.
4. Electrical impedance was also measured while loading the specimen. Piezoresistive based sensitivity of various samples were evaluated based on test results.
5. Based on the modeling of the behavior, the proposed p-q model predicted the piezoresistive and curing behavior of behavior of both modified and unmodified smart cement.
6. The artificial intelligence models will be used to predict the experimental results.

CHAPTER 4 SMART CEMENT

4.1 Introduction

This section involves laboratory characterization of smart cement in both slurry and hardened state for a period of 28 days. The smart cement is characterized using electrical resistivity, electrical impedance, compressive strength and piezoresistivity.

Effect of various additives has been investigated on the Sensitivity of Smart cement. This chapter has been subdivided into three sub sections to highlight the effect of additive on smart cement. Although similar tests and procedures have been followed for quantifying the effect of additives, the materials, research methodology implemented, and models used has been included inside each sub chapter separately. The following subchapters under this subsection are as follows.

1) Standard Smart Cement Mix used as a baseline for further tests.
2) Effect of Salt contamination on the Electrical properties, Compressive strength and Piezoresistive behavior of Smart Cement.
3) Effect of Salt contamination on the Electrical properties, Compressive strength and Piezoresistive behavior of Smart Cement.
4) Moisture Detection Sensitivity of Smart Cement.

Commercially available oil well cement (Class H cement) was modified with conductive fillers to make it a piezoresistive material. The Cement was modified by adding about 0.04% of conductive filler (CF), by weight of cement, and the water to cement ratio was 0.4.

4.2 k Value Characterization

In slurry state, the Resistance and Resistivity values were measured using an LCR and Conductivity probe respectively, for upto 220 mins. Relation between Resistance, Resistivity and k value is given by: $\rho = \frac{R}{K + GR}$. (**4.1**)

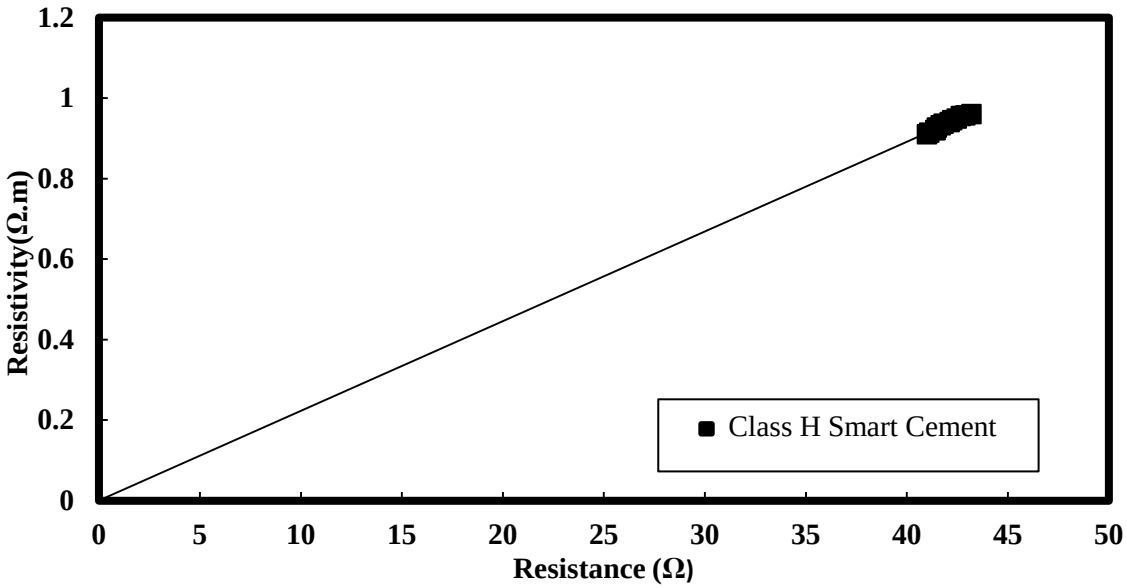

Figure – 4.1 Electrical Resistance vs Electrical Resistivity Plot for Smart Cement

Electrical resistance and electrical resistivity have a linear relationship for smart cement (Figure – 4.1). Electrical resistance and electrical resistivity increase with time when cured under room temperature whereas k value remains constant (Figure – 4.2). The average value of k is 44.98/m

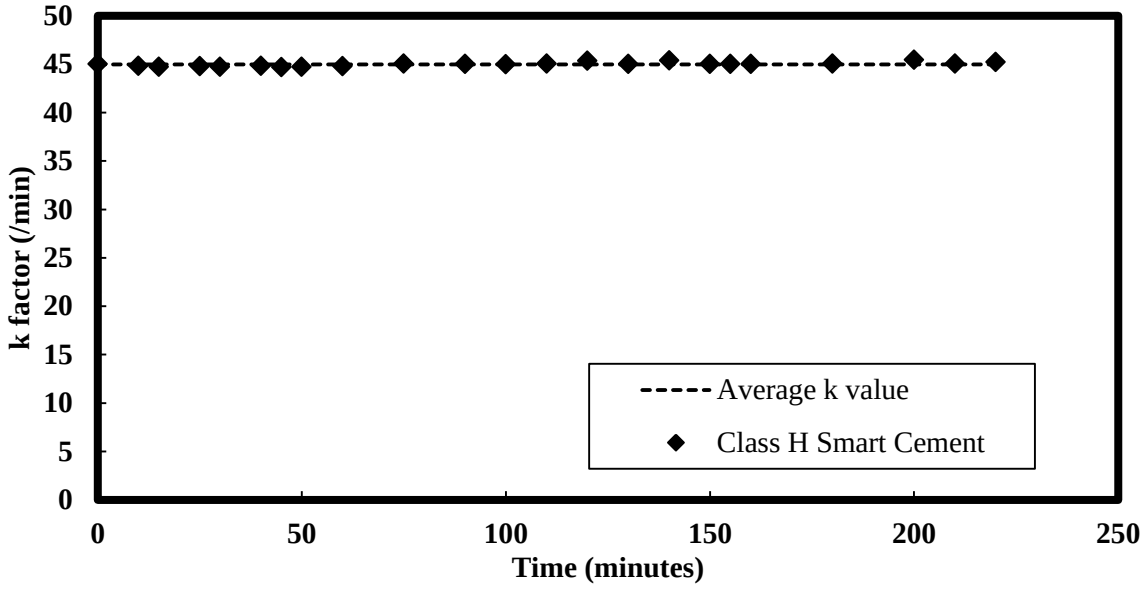

Figure – 4.2(a) Variation of k with time

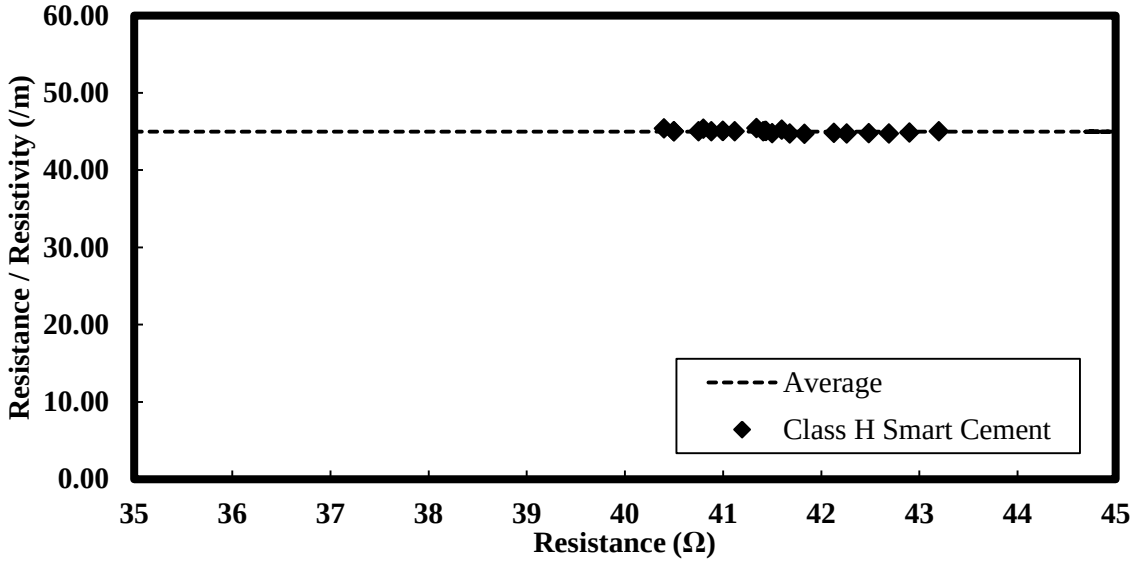

Figure – 4.2(b) Electrical Resistance/Electrical Resistivity (R/ρ) vs Electrical Resistance for Smart Cement.

4.3 Impedance vs Frequency Curves

Electrical Impedance is calculated using the following equation:

$$Z = [(R^2 + X^2)^{½}] \qquad (4.2)$$

Here, R and X are noted from an LCR at different frequencies.

Following are the Impedance curves for Smart Cement at 1 and 28 days of curing.

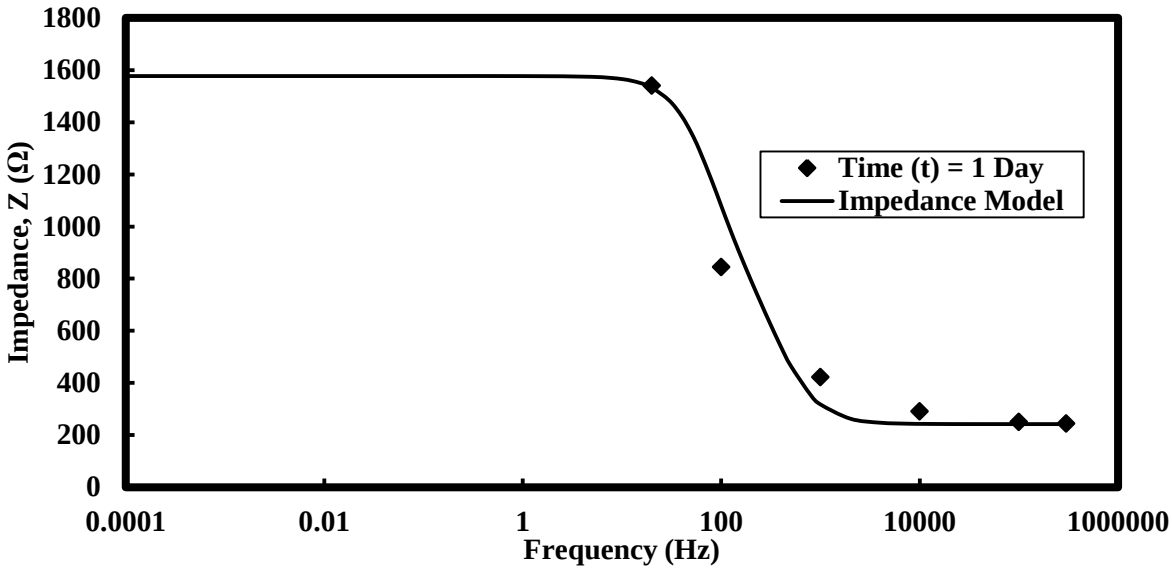

Figure – 4.3 Electrical Impedance curve for Smart Cement at 1day of curing

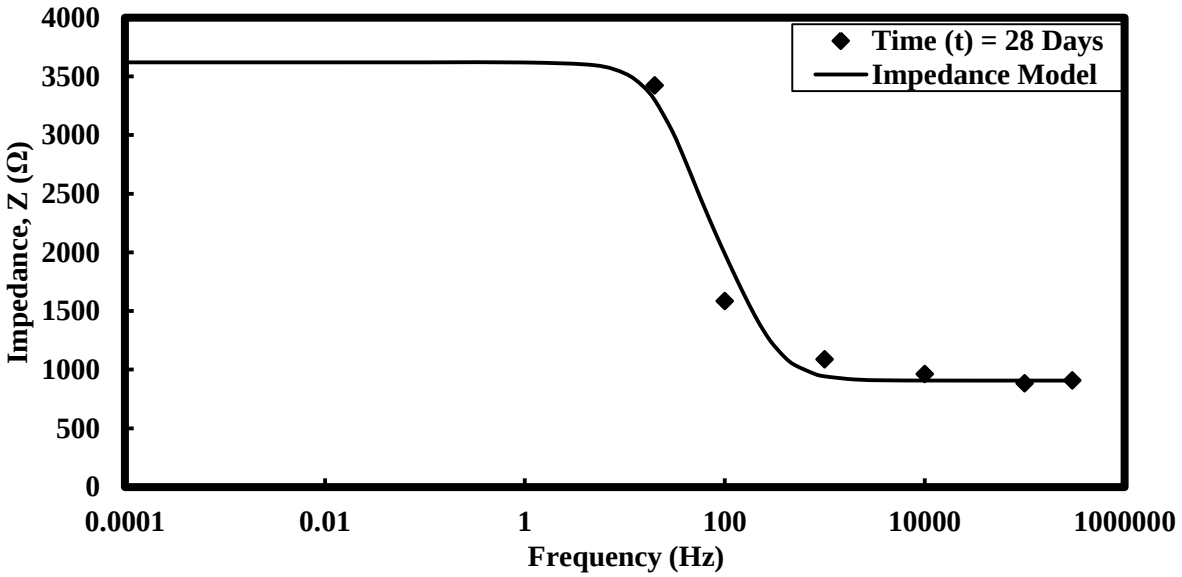

Figure – 4.4 Electrical Impedance curve for Smart Cement at 28days of curing

Table – 4.1 Resistance and Capacitance for Smart Cement at 1 and 28 days of curing

DAYS OF CURING	Rc_1 (Ω)	Cc_1 (F)	Rc_2 (Ω)	Cc_2 (F)	R_b (Ω)	R^2	RMSE (Ω)
1	7.75E+02	2.49E-06	5.60E+02	7.50E-07	242	0.95	1.07E+02
28	1.56E+03	2.53E-06	1.15E+03	6.00E-07	907	0.96	1.84E+02

Rc_1 and Rc_2 represent contact resistances, R_b represents bulk resistance, Cc_1 and Cc_2 represent contact capacitances. Here, impedance versus frequency relationship shows that the smart cement sample follows case 2 behavior (Figure – 3.7), indicating that the bulk material can be represented by resistance at high frequency impedance measurement.

4.4 Electrical Resistivity

After the cement mix was poured into the mold, initial resistivity (ρ_o = 0.96 Ω m) was noted. Resistance values were taken by LCR meter for up to 240 minutes. Resistivity dipped initially indicating the formation of large amounts of hydration products in cement matrix. Change in the electrical resistivity with respect to minimum resistivity quantifies

the formation of hydration products, which leads to shrinkage and development of cement strength. Thereby by monitoring the change in resistivity of the cement slurry, a clear understanding of the hydration process and strength development can be obtained. (Vipulanandan & Mohammed, 2015).

Electrical Resistivity is used as a parameter used to monitor and characterize the curing process of cement. As the cement cures, resistivity changes with time. During the curing process, parameters such as initial resistivity (ρ_o), minimum resistivity (ρ_{min}), time required to reach minimum resistivity (t_{min}), are monitored.

4.4.1 Smart Cement prepared with tap water

It is observed that, after the cement is mixed, resistivity first decreases to reach minimum resistivity and then gradually increases with time (Figure – 4.5). Time required to reach minimum resistivity can be used as an indicator to monitor the setting time of cement. The formation of hydration products obstructs the flow of current, and hence the resistivity increases with time. The electrical resistivity was modeled using Vipulanandan electrical resistivity model (Eqn. 3.5)

1 Day Curing

The normal trend of the resistivity during the curing of cement is that the resistivity decreases up to a certain time (t_{min}) to reach the minimum resistivity (ρ_{min}) and then increases with time. The value of initial resistivity of smart cement was 0.96 Ω.m. immediately after mixing, which can be used as a quality control measure in the field. The value of minimum resistivity was 0.89 Ω.m. and the time for minimum resistivity was 130 minutes after mixing. The resistivity after 1 day of curing was 3.38 Ωm (Table – 4.8).

For training the AI models with one, two, three and four layers of ANN were used with the GRNN approach. Based on the training results, four layer AI model was selected to predict the smart cement curing trend using the AI model and compare it to the Vipulanandan Curing Model.

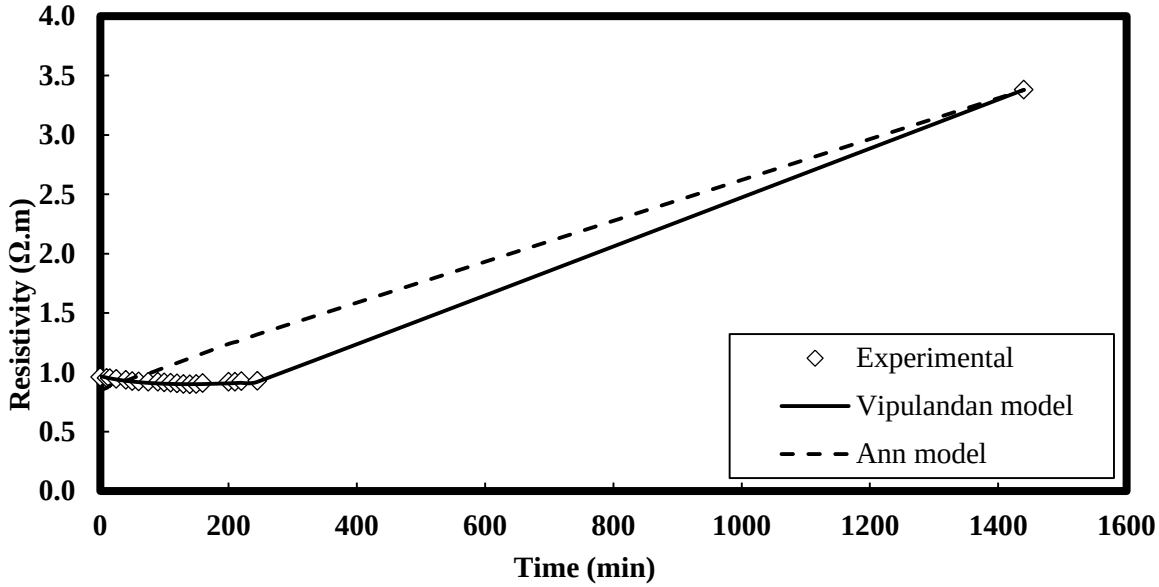

Figure – 4.5 Electrical Resistivity of Smart Cement for 1 day of curing

Vipulandan Model parameters; p1 and q1 are 0.03 and 0.09 respectively, the coefficient of determination (R^2) is 0.99 and the RMSE (root mean square error) is 0.07 Ωm (Table – 4.2). Also, AI model prediction is compared to the experimental data (Figure – 4.5), the coefficient of determination (R^2) was 0.98 and the RMSE (root mean square error) was 0.2 Ωm (Table – 4.3).

28 Day Curing

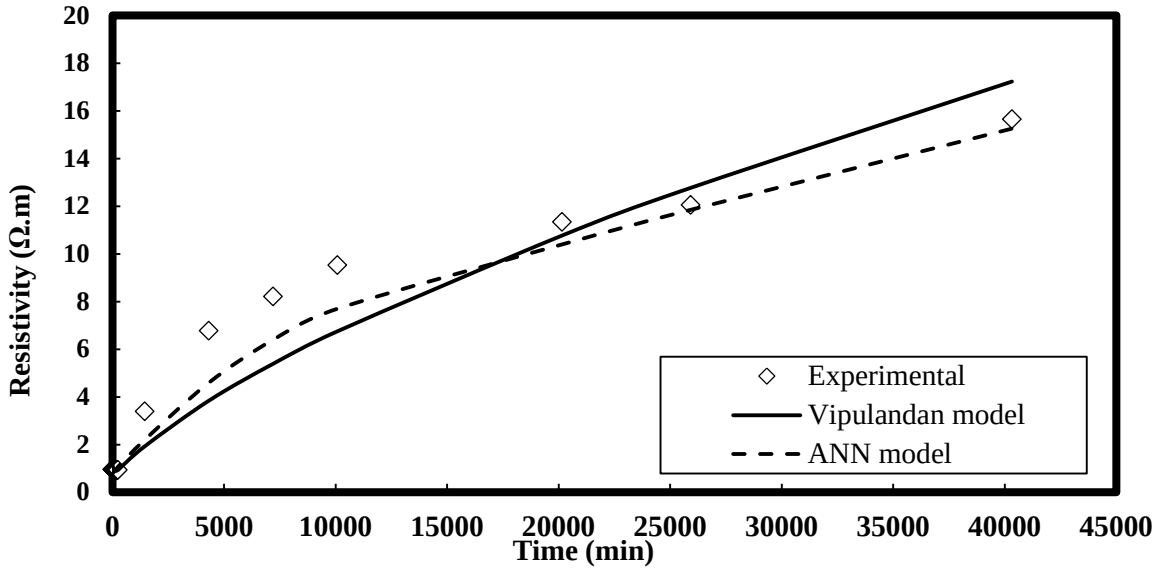

Figure – 4.6 Electrical Resistivity of Smart Cement for 28 days of curing

Resistivity after 28 days of curing is 15.64 Ωm (Figure – 4.6), which is 1529% higher than initial resistivity (ρ_o) and 362% higher than resistivity at 1 day of curing. This shows the sensitivity of smart cement to curing behavior.

Vipulandan Model parameters; p1 and q1 are 0.59 and 0.4 respectively, the coefficient of determination (R^2) is 0.99 and the RMSE (root mean square error) is 0.97 Ωm (Table – 4.2). Also, AI model prediction is compared to the experimental data (Figure – 4.6), the coefficient of determination (R^2) was 0.94 and the RMSE (root mean square error) was 0.98 Ωm (Table – 4.3).

Table – 4.2 Electrical Resistivity Model parameters for smart cement

CURING DAYS	p_1	q_1	R^2	RMSE (Ω m)
1	0.03	0.09	0.99	0.07
28	0.59	0.4	0.99	0.97

Table – 4.3 Comparison of Vipulanandan Resistivity Model and ANN Model for Smart Cement

CURING DAYS	CURING MODEL		ANN MODEL	
	R^2	RMSE (Ω m)	R^2	RMSE (Ω m)
1	0.99	0.07	0.98	0.2
28	0.99	0.97	0.94	0.98

4.4.2 Smart Cement prepared with salty water

The objective was to monitor and understand the electrical and piezoresistive properties of salt contaminated smart cement in slurry and hardened state and to differentiate them with that of standard cement grout. Smart cement was prepared from salt water (Salinity 35gm/L).

1 Day Curing

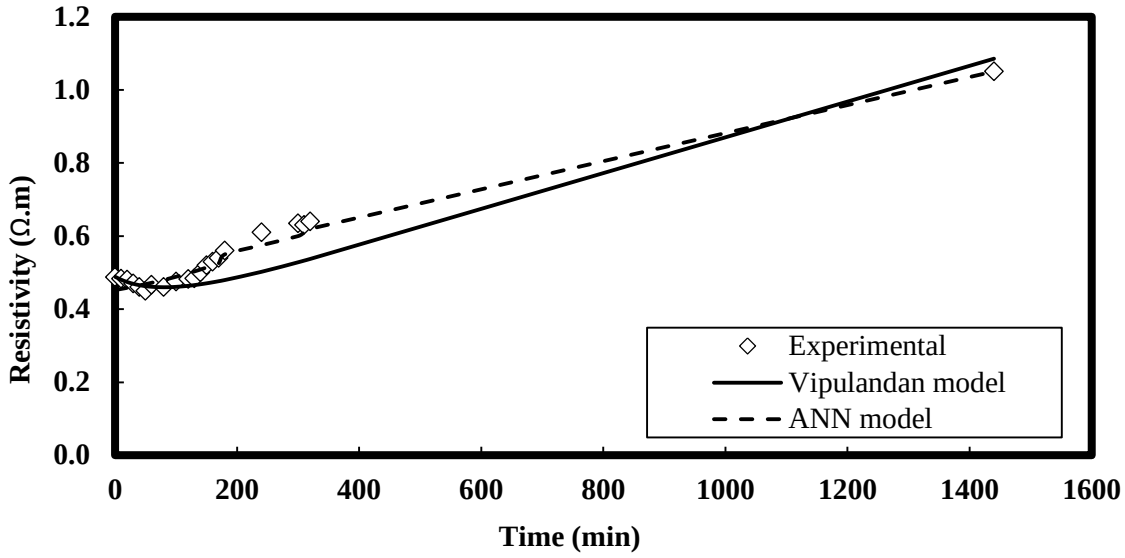

Figure – 4.7 Electrical Resistivity of Smart Cement with salt water for 1 day of curing

It was observed that salt contamination reduces the initial resistivity (ρ_o) to 0.487Ω m from 0.96 Ωm (Table – 4.8) for standard smart cement grout thereby also accelerating the hydration time from 130 mins to 80mins.

Vipulandan Model parameters; p1 and q1 are 0.57 and 0.42 respectively, the coefficient of determination (R^2) is 0.99 and the RMSE (root mean square error) is 0.05 Ωm (Table – 4.4). Also, AI model prediction is compared to the experimental data (Figure – 4.7), the coefficient of determination (R^2) was 0.97 and the RMSE (root mean square error) was 0.02 Ωm (Table – 4.5).

28 Day Curing

Resistivity after 28 days (ρ_{28}) of curing is 2.36 Ωm (Table – 4.8), which is 384% higher than initial resistivity (ρ_o) and 124% higher than resistivity at 1 day of curing.

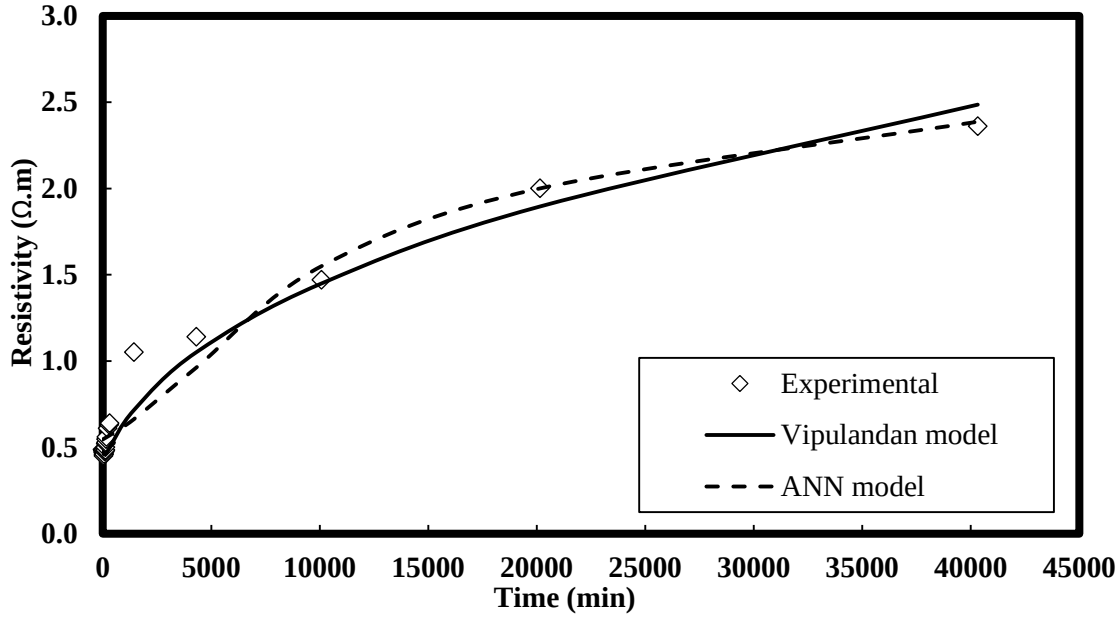

Figure – 4.8 Electrical Resistivity of Smart Cement with salt water for 28 days of curing

Vipulandan Model parameters; p1 and q1 are 0.71 and 0.28 respectively, the coefficient of determination (R^2) is 0.99 and the RMSE (root mean square error) is 0.09 Ωm (Table – 4.4). Also, AI model prediction is compared to the experimental data (Figure – 4.8), the coefficient of determination (R^2) was 0.91 and the RMSE (root mean square error) was 0.11 Ωm (Table – 4.5).

Table – 4.4 Electrical Resistivity Model parameters for smart cement with salt water

CURING DAYS	p_1	q_1	R^2	RMSE (Ω m)
1	0.57	0.42	0.99	0.05
28	0.71	0.28	0.99	0.09

Table – 4.5 Comparison of Vipulanandan Resistivity Model and ANN Model for Smart Cement with salt water

CURING DAYS	CURING MODEL		ANN MODEL	
	R^2	RMSE (Ω m)	R^2	RMSE (Ω m)
1	0.99	0.05	0.94	0.82
28	0.99	0.09	0.91	0.11

4.4.3 Smart Cement prepared with UH-Biosurfactant (UH-BS)

The objective was to monitor the effect of UH-BS on the electrical and piezoresistive properties of smart cement for upto 28 days of curing by adding 1.25% of UH-BS by weight of cement (bwoc). Smart cement specimen was prepared with w/c = 0.35.

1 Day Curing

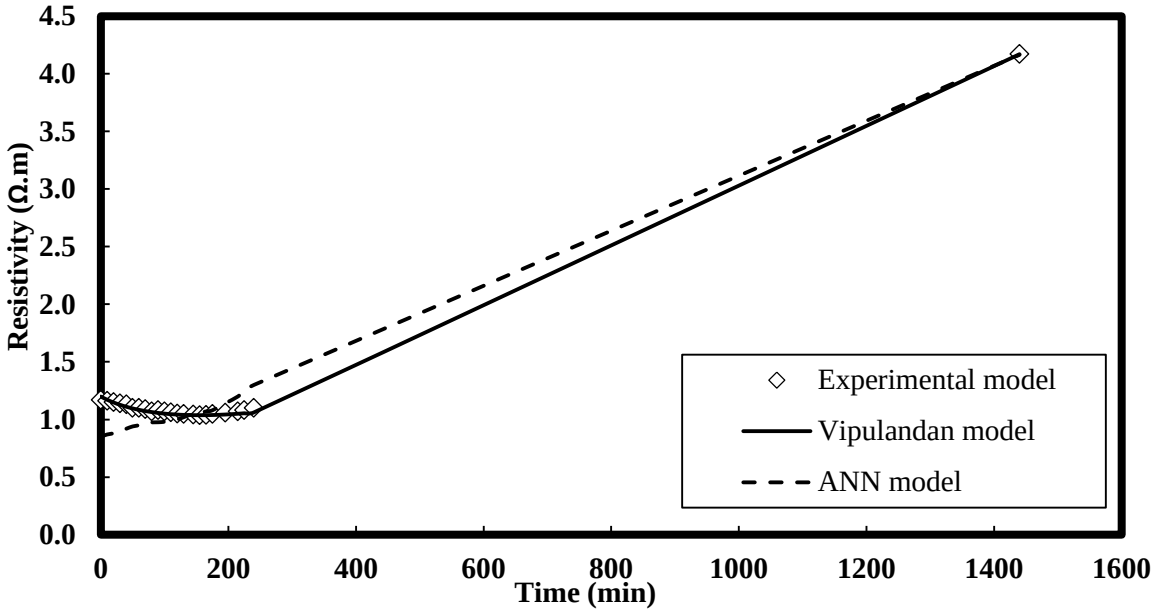

Figure – 4.9 Electrical Resistivity of Smart Cement with UH-BS for 1 day of curing

It was observed that addition of Bio-surfactant increase the initial resistivity (ρ_o) to 0.1.17Ω m from 0.96 Ωm (Table – 4.7) for standard smart cement grout thereby also increasing the hydration time from 130 minutes to 155 minutes.

Vipulandan Model parameters; p1 and q1 are 0.1 and 0.21 respectively, the coefficient of determination (R^2) is 0.99 and the RMSE (root mean square error) is 0.01 Ωm (Table – 4.6). Also, AI model prediction is compared to the experimental data (Figure – 4.9), the coefficient of determination (R^2) was 0.95 and the RMSE (root mean square error) was 0.16 Ωm (Table – 4.7).

28 Day Curing

Resistivity after 28 days (ρ_{28}) of curing is 34.36 Ωm (Table – 4.8), which is 124% higher than resistivity at 1 day of curing.

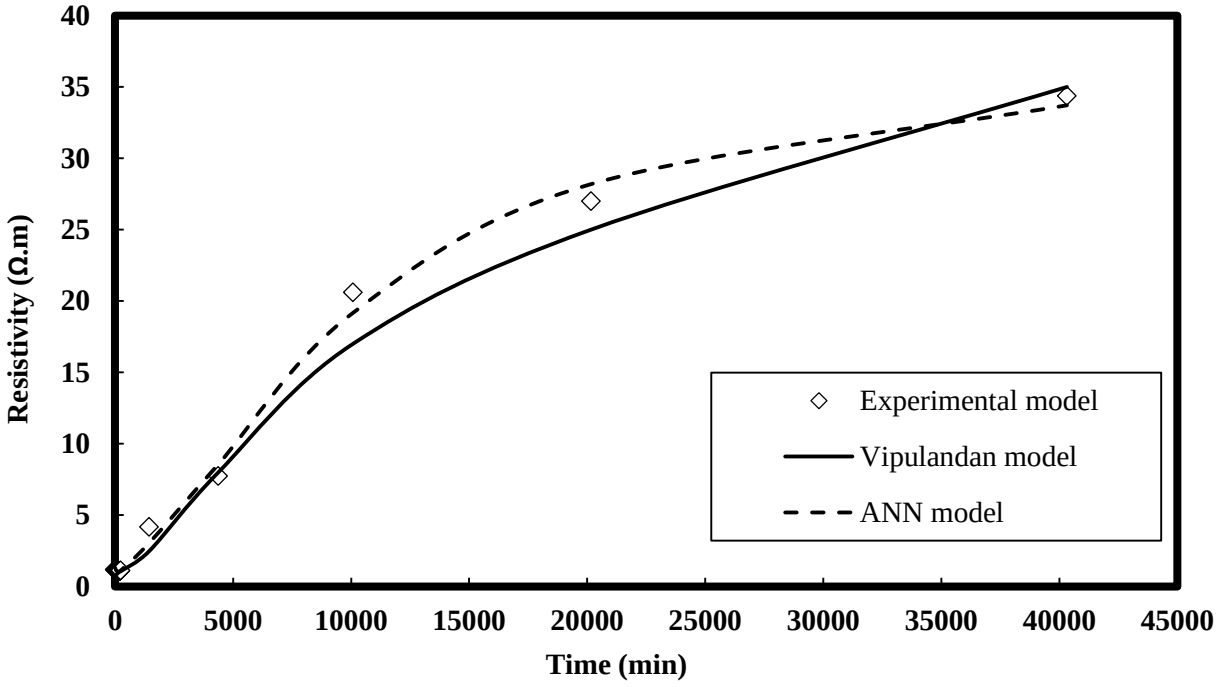

Figure – 4.10 Electrical Resistivity of Smart Cement with UH-BS for 28 days of curing

Vipulandan Model parameters; p1 and q1 are 0.0.53 and 0.46 respectively, the coefficient of determination (R^2) is 0.99 and the RMSE (root mean square error) is 0.85 Ωm (Table – 4.6). Also, AI model prediction is compared to the experimental data (Figure – 4.10), the coefficient of determination (R^2) was 0.91 and the RMSE (root mean square error) was 0.51 Ωm (Table – 4.7).

Table – 4.6 Electrical Resistivity Model parameters for smart cement with UH-Biosurfactant

CURING DAYS	p_1	q_1	R^2	RMSE (Ω m)
1	0.1	0.21	0.99	0.01
28	0.53	0.46	0.99	0.85

Table – 4.7 Comparisons of Vipulanandan Resistivity Model and ANN Model for Smart Cement with UH-BS

CURING DAYS	CURING MODEL		ANN MODEL	
	R^2	RMSE (Ω m)	R^2	RMSE (Ω m)
1	0.99	0.01	0.94	0.16
28	0.99	0.85	0.91	0.51

Comparison of Electrical properties

Table – 4.8 Comparisons of Electrical Resistivity parameters for smart cement with additives

SMART CEMENT	Initial Resistivity ρ_o (Ωm)	Minimum Resistivity ρ_{min} (Ωm)	t_{min} (min)	ρ_1 (Ωm)	ρ_{28} (Ωm)
Tap water	0.96 ± 0.03	0.89 ± 0.01	130 ± 5	3.38 ± 0.02	15.64 ± 0.04
Salt water	0.487 ± 0.04	0.45 ± 0.01	55 ± 5	1.05 ± 0.04	2.36 ± 0.06
UH-BS	1.17 ± 0.02	1.03 ± 0.01	155 ± 5	4.17 ± 0.03	34.36 ± 0.04

For Standard Smart Cement grout (prepared with tap water); initial resistivity (ρ_o) and minimum resistivity (ρ_{min}) was 0.96 Ωm and 0.89 Ωm respectively (Table – 4.8).

For Smart Cement prepared with salt water; Initial Resistivity (ρ_o) and Minimum Resistivity (ρ_{min}) was 0.487 Ωm and 0.45 Ωm respectively. Addition of salt decreases the initial resistivity by 97% and minimum resistivity by 93% as compared to Smart Cement prepared with tap water (Table – 4.8). Similar trend was observed for 1 day resistivity and 28 day resistivity. 1 day resistivity decreased to 1.05 Ωm (decrease of about 221%) and 28 day resistivity to 15.64 Ωm (decrease of about 562%) as compared to those of smart cement with tap water (Table – 4.8). Also, the time required to reach minimum resistivity decreased from 130 minutes to 55 minutes (Table – 4.8), thereby indicating that there has been acceleration in the setting time of cement due to the addition of salt.

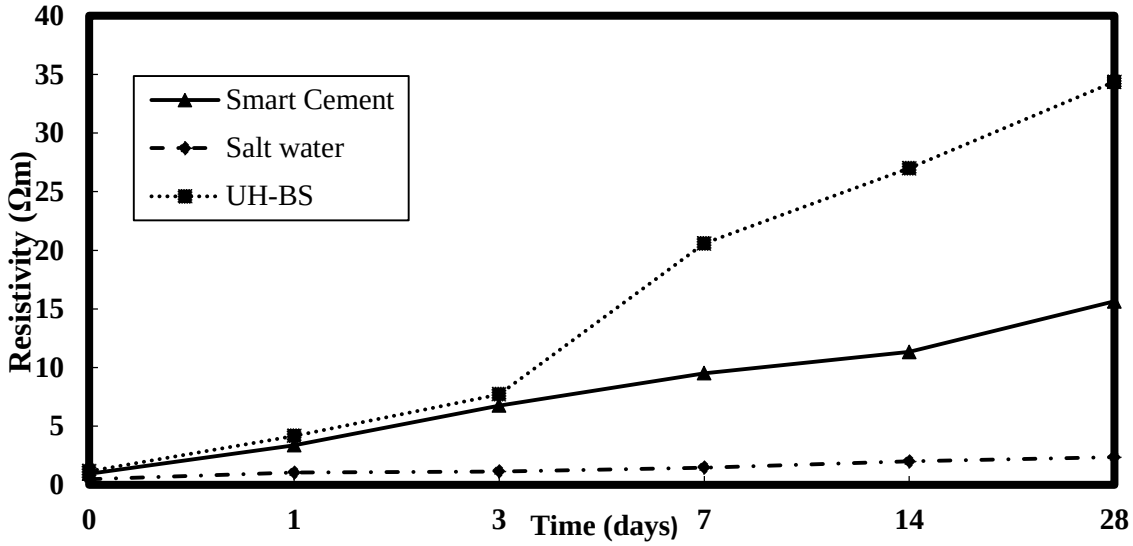

Figure – 4.11 Comparison of Electrical Resistivity of Smart Cement with additives

For Smart Cement prepared with UH-BS; initial resistivity (ρ_o) and minimum resistivity (ρ_{min}) was 1.17 Ωm and 1.03 Ωm respectively (Table – 4.8). Addition of UH-BS increases the initial resistivity by 22% and minimum resistivity by 16% as compared to Smart Cement prepared with tap water (Table – 4.8). Similar trend was observed for 1 day resistivity and 28 day resistivity. 1 day resistivity increased to 4.17 Ωm (increase of about 23%) and 28 day resistivity to 34.36 Ωm (increase of about 120%) as compared to those of smart cement with tap water (Table – 4.8). Also, the time required to reach minimum resistivity increased from 130 minutes to 155 minutes (Table – 4.8), thereby indicating that there has been retardation in the setting time of cement due to the addition of UH-BS.

Shrinkage

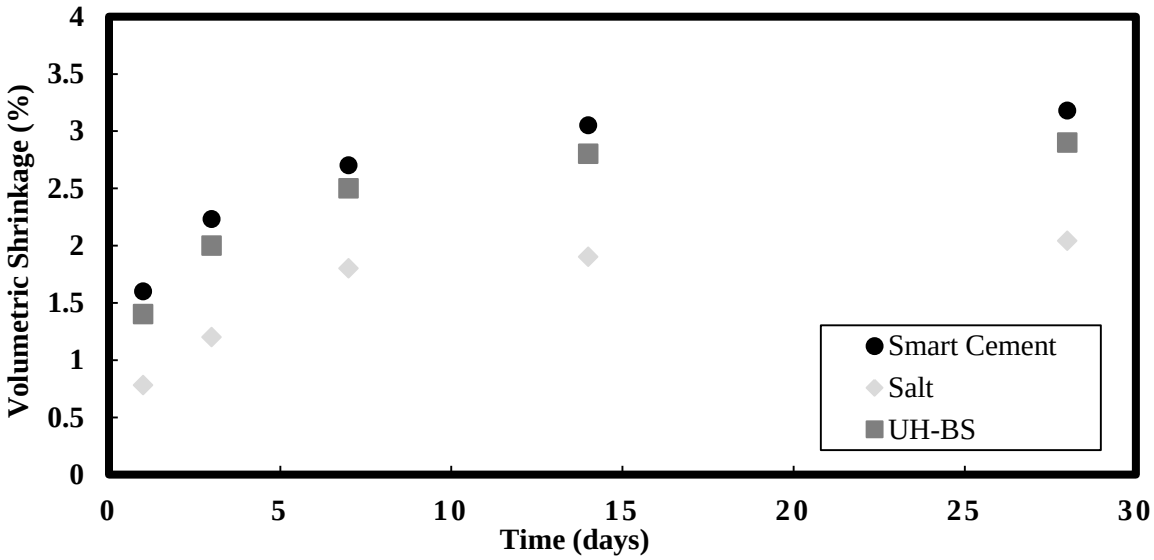

Figure – 4.12 Shrinkage of Smart Cement with and without additives

Smart Cement specimens prepared with tap water undergo volumetric shrinkage of about 3.18% in 28 days of curing. Salt and UH-BS addition help to reduce the shrinkage to 2% and 2.9% respectively.

4.5 Piezoresistivity

To quantify the piezoresistive behavior of hardened smart cement, specimens were demolded after 24 hours and cured in room temperature for 28 days. Specimens were then tested under compressive stress and the change in resistivity was recorded. Change in resistivity due to application of stress is called as the *Piezoresistive behavior* of smart cement.

4.5.1Smart Cement prepared with tap water

The piezoresistive strain for smart cement sample was 201 % at a peak compressive stress of 9.3 MPa (1550 psi) after 1 day of curing. Hence, the piezoresistivity per unit stress was 0.13%/psi in the lab samples after 1 day of curing. The piezoresistive strain for smart cement sample was 205 % at a peak compressive stress of 21.24 MPa (3200 psi) after 28 days of curing.

Hence, the piezoresistivity per unit stress was 0.058%/psi in the lab samples after 28 days of curing.

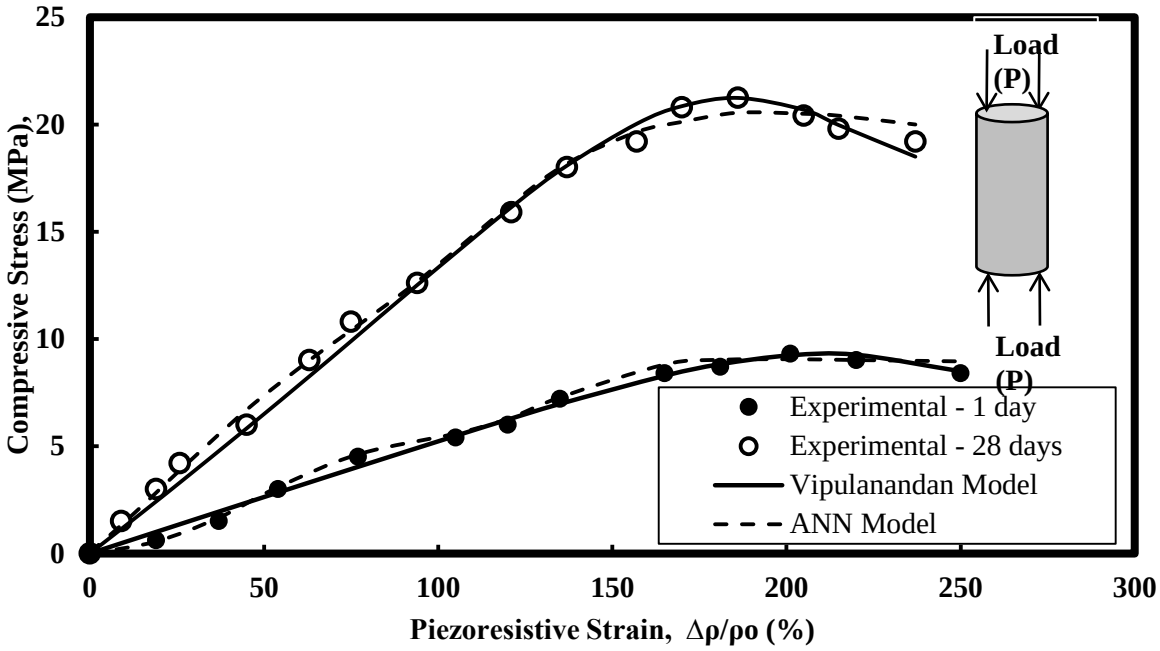

Figure – 4.13 Piezoresistive Behavior of Smart Cement for 28 days of curing.

Table – 4.9 Comparisons of Piezoresistivity Model and ANN Model for Smart Cement with tap water

CURING DAYS	PIEZORESISTIVITY MODEL		ANN MODEL	
	R^2	RMSE (MPa)	R^2	RMSE(MPa)
1	0.99	0.34	0.99	0.65
28	0.99	0.5	0.98	0.44

Short term (1 day) and long term (28 days) piezoresistive behavior was predicted very well by the piezoresistive model and the ANN model.

For 1 day of curing the coefficient of determination (R^2) was 0.99 for both the models whereas root mean square (RMSE) values were 0.34 Mpa and 0.25 Mpa for piezoresistivity and ANN model respectively. For 28 days of curing the coefficient of determination (R^2) was 0.99 and 0.98 for piezoresistivity model and ANN model respectively whereas the root mean square

(RMSE) values were 0.5 Mpa and 0.44 Mpa for piezoresistivity model and ANN model respectively (Table – 4.9).

4.5.2 Smart Cement prepared with salty water

The piezoresistive strain for smart cement sample was 164 % at a peak compressive stress of 13.50 Mpa (2250 psi) after 1 day of curing. Hence, the piezoresistivity per unit stress was 0.07%/psi in the lab samples after 1 day of curing. The piezoresistive strain for smart cement sample was 97 % at a peak compressive stress of 22.2 Mpa (3700 psi) after 28 days of curing. Hence, the piezoresistivity per unit stress was 0.026%/psi in the lab samples after 28 days of curing.

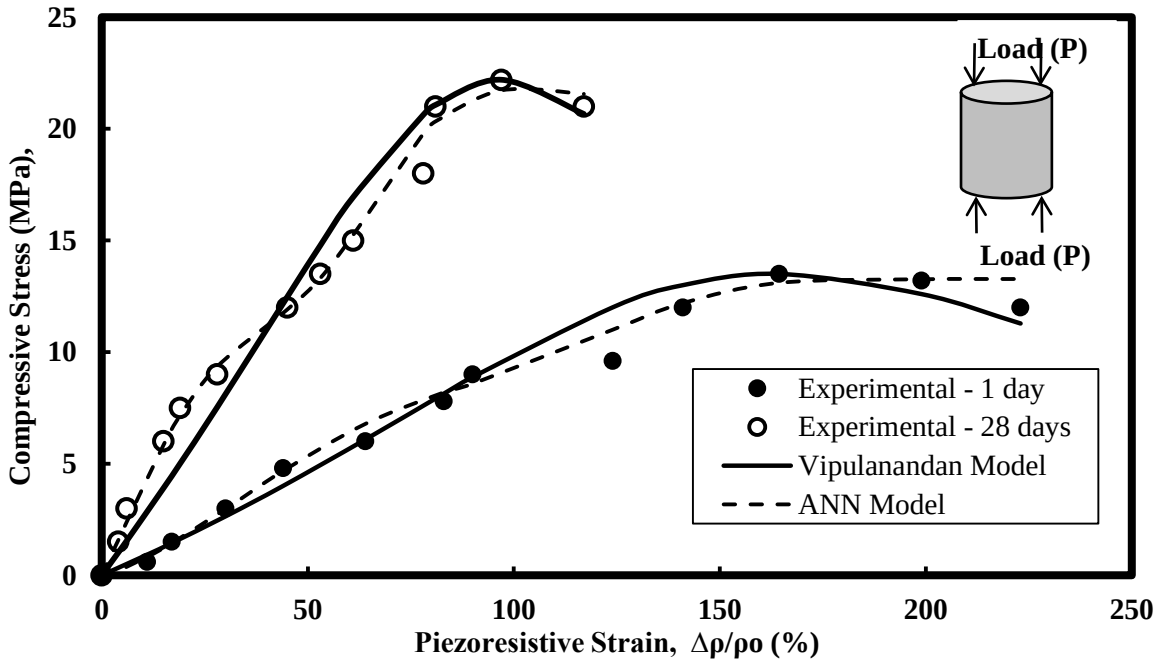

Figure – 4.14 Piezoresistive Behavior of Smart Cement with salt water for 28 days of curing.

Table – 4.10 Comparison of Piezoresistivity Model and ANN Model for Smart Cement with salt water

CURING DAYS	PIEZORESISTIVITY MODEL		ANN MODEL	
	R^2	RMSE (MPa)	R^2	RMSE (MPa)
1	0.99	0.53	0.97	0.37
28	0.99	0.82	0.99	0.42

For 1 day of curing the coefficient of determination (R^2) was 0.99 and 0.97 whereas root mean square (RMSE) values were 0.53 Mpa and 0.37 Mpa for piezoresistivity and ANN model

respectively. For 28 days of curing the coefficient of determination (R^2) was 0.99 for both, piezoresistivity model and ANN model whereas the root mean square (RMSE) values were 0.82 Mpa and 0.42 Mpa for piezoresistivity model and ANN model respectively (Table 4-10).

4.5.3 Smart Cement prepared with UH-BS

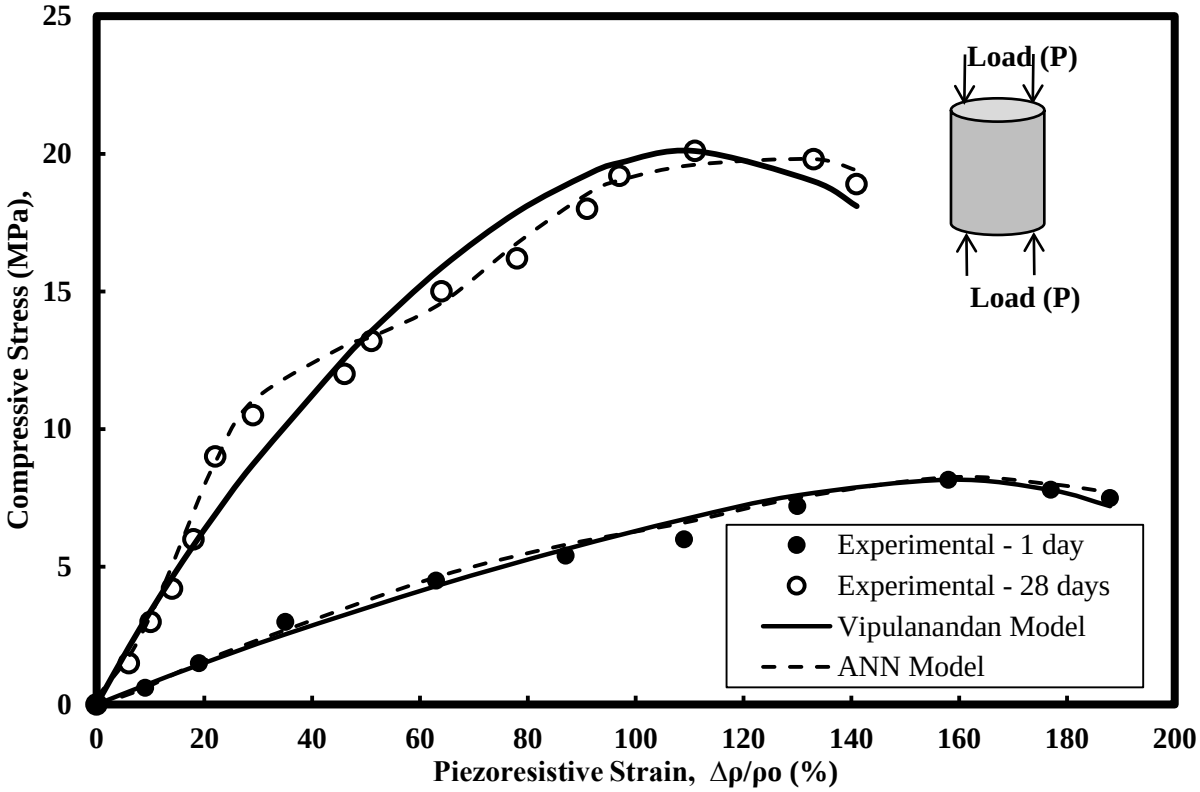

Figure – 4.15 Piezoresistive Behavior of Smart Cement with UH-BS for 28 days of curing.

The piezoresistive strain for smart cement sample was 158 % at a peak compressive stress of 8.16 Mpa (1360 psi) after 1 day of curing. Hence, the piezoresistivity per unit stress was 0.11%/psi in the lab samples after 1 day of curing. The piezoresistive strain for smart cement sample was 111 % at a peak compressive stress of 21 Mpa (3500 psi) after 28 days of curing. Hence, the piezoresistivity per unit stress was 0.03%/psi in the lab samples after 28 days of curing.

Table – 4.11 Comparisons of Piezoresistivity Model and ANN Model for Smart Cement with UH-BS

CURING DAYS	PIEZORESISTIVITY MODEL		ANN MODEL	
	R^2	RMSE (MPa)	R^2	RMSE (MPa)
1	0.99	0.31	0.98	0.42
28	0.98	0.39	0.97	0.28

For 1 day of curing the coefficient of determination (R^2) was 0.99 and 0.98 whereas root mean square (RMSE) values were 0.31 Mpa and 0.11Mpa for piezoresistivity and ANN model respectively. For 28 days of curing the coefficient of determination (R^2) was 0.99 and 0.97 whereas the root mean square (RMSE) values were 0.39 Mpa and 0.28 Mpa for piezoresistivity model and ANN model respectively (Table 4-11).

Table – 4.12 Piezpresistivity Model parameters for smart cement with and without additives

	1 DAY				28 DAYS			
	p2	**q2**	**R^2**	**RMSE**	**p2**	**q2**	**R^2**	**RMSE**
TAP WATER	0.19	0.8	0.99	0.34	0.2	0.9	0.99	0.5
SALT WATER	0.22	0.77	0.98	0.53	0.16	0.64	0.99	0.82
UH-BS	0.65	0.08	0.99	0.31	0.1	0.50	0.98	0.39

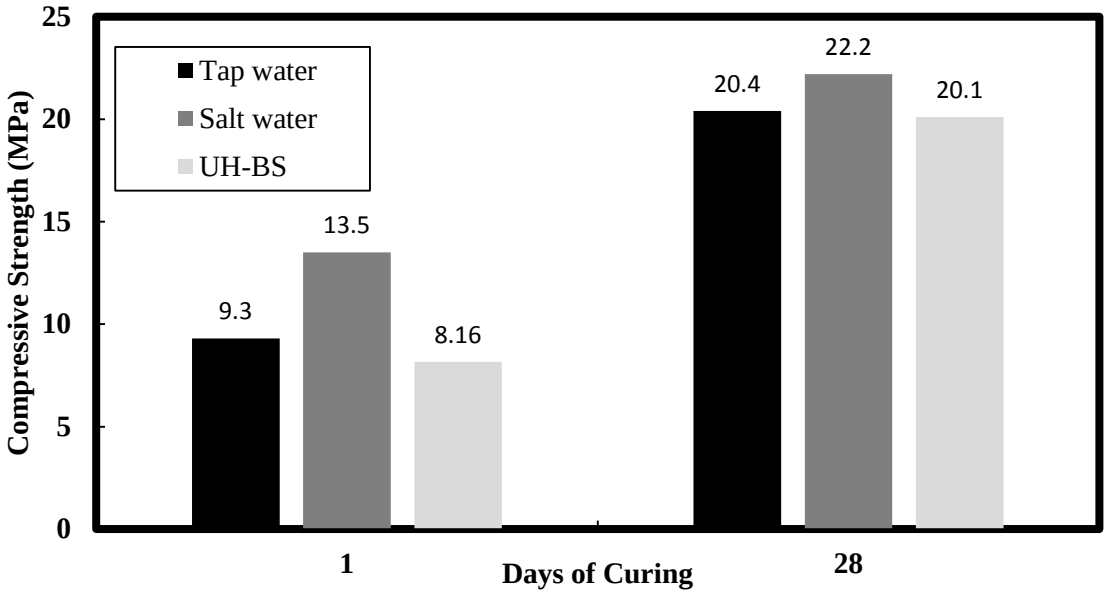

Figure – 4.16 Variation of Compressive Strength of Smart Cement with and without additives for 28 days of curing.

Addition of Salt has increased the short term (1 day) and long term (28 days) compressive strength of smart cement specimen by about 45% and 9% respectively (Figure – 4.16) as compared to that of Smart Cement with tap water. Whereas, addition of UH-BS decreases the short term compressive strength by about 12% whereas the long term compressive strength remains almost the same as Smart Cement with tap water (Figure – 4.16).

4.6 Moisture Detection Sensitivity of Smart Cement

The objective was to monitor and understand the changes in electrical properties of smart cement specimen due to the penetration of tap water and saline water. In this study, smart cement samples were prepared with water to cement ratio of 0.4 and 0.05% of conductive filler. Initially samples were immersed upto 0.5" depth (Figure – 4.17(a)) and changes in the electrical properties were noted; followed by raising the water level to 2" depth (Figure – 4.17(b)). Similar tests were conducted for different specimens immersed in tap water and saline water (Salinity 35gm/L).

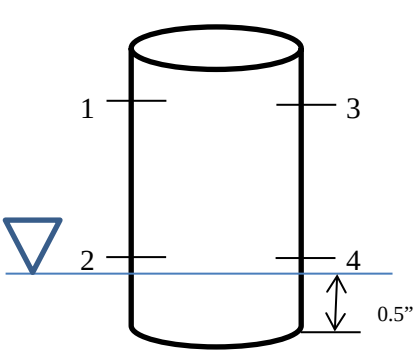

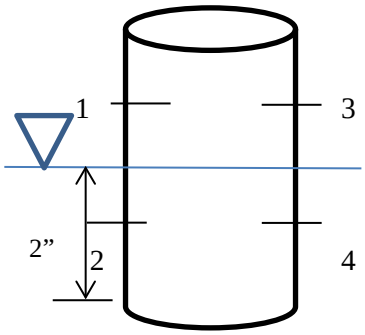

Figure – 4.17 (a) sample immersed upto 0.5” **(b) sample immersed upto 2”**

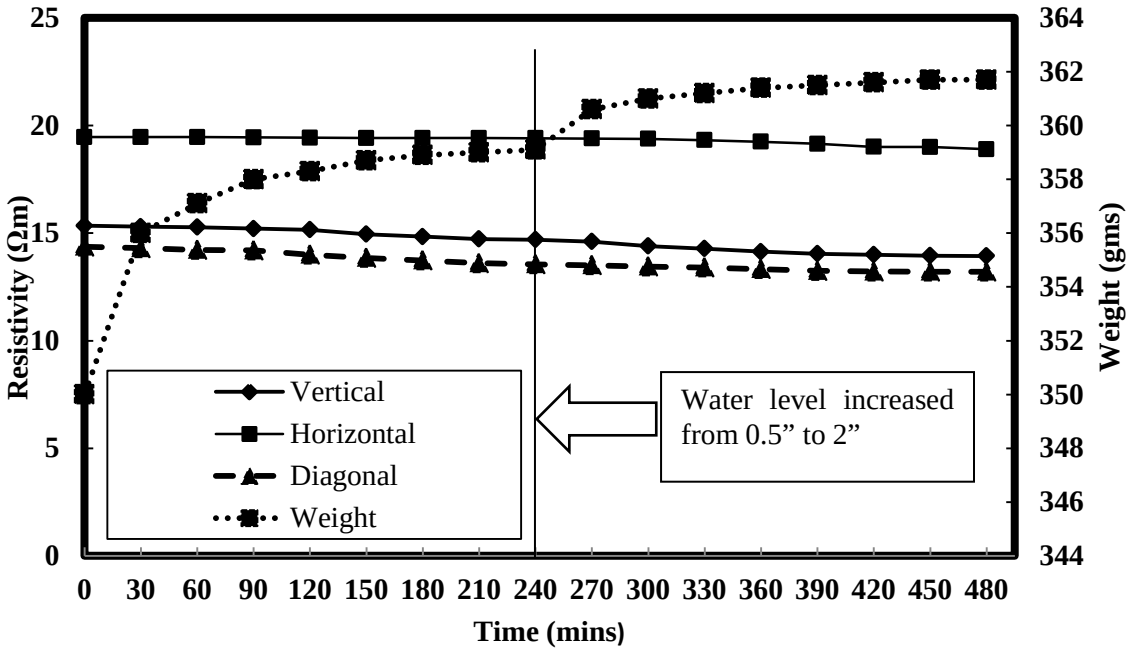

Figure – 4.18 Variation in Resistivity and weight with time for specimen dipped in tap water

It can be seen that (Figure – 4.18 and 4.19), due to submergence of smart cement sample in the water, electrical resistivity decreases whereas the weight of specimen increases. Though electrical resistivity decreases in all directions but the rate of change varies.

For the first 240 minutes, the water level was below combination 2-4, so resistivity of horizontal combination (combination 1-3) did not change considerably as compared to resistivity of vertical (combination 1-2) and diagonal (combination 1-4) combinations (Figure – 4.18).

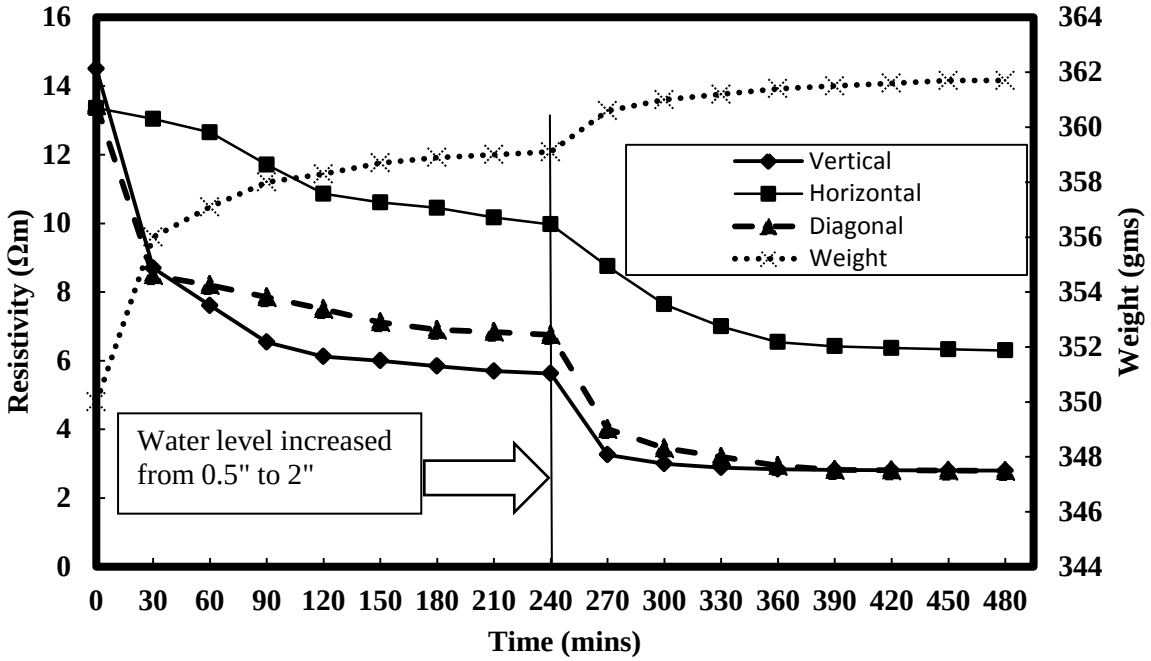

Figure – 4.19 Variation in Resistivity and weight with time for specimen dipped in salty water

Table – 4.13 Change in properties of smart cement due to different submergence conditions.

Water	After 240 minutes				After 480 minutes			
	Vertical Resistivity (%)	Horizontal Resistivity (%)	Diagonal Resistivity (%)	Weight (%)	Vertical Resistivity (%)	Horizontal Resistivity (%)	Diagonal Resistivity (%)	Weight (%)
Tap water	-4	-0.27	-5	2	-9	-3	-8	3
Salt water	-58	-25	-49	7	-82	-53	-80	14

Table – 4.13 represents the change in the directional electrical resistivity and weight of the smart cement specimen when immersed in tap water and salty water. Due to infiltration of water in the specimen, electrical resistivity decreases whereas weight of the sample increases.

For the specimen immersed in tap water, intial resistivity of vertical, horizontal and diagonal combinations was 15.34 Ωm, 19.46 Ωm and14.37 Ωm respectively (Figure – 4.18).

After 480 minutes of submergence, resistivity of vertical, horizontal and diagonal combinations reduced by 9%, 3% and 8% respectively, along with 3% increase in the weight of specimen (Table – 4.18). For the specimen immersed in salty water, intial resistivity of vertical, horizontal and diagonal combinations was 14.5 Ωm, 13.36 Ωm and 13.44Ωm respectively (Figure – 4.19). After 480 minutes of submergence, resistivity of vertical, horizontal and diagonal combinations reduced by 82%, 53% and 80% respectively, along with 14% increase in the weight of specimen (Table – 4.19).

Moisture content could be determined on the basis of electrical resistivity of Smart Cement specimen (Figure – 4.20). Also there is a considerable difference in the resistivity due to the addition of salt as compared to that of tap water.

Changes in Resistivity could be due to the diffusion of liquids due to concentration gradient or due to capillary rise of water. Salt infusion could also cause chemical reactions thereby leading to considerable decrease in resistivity.

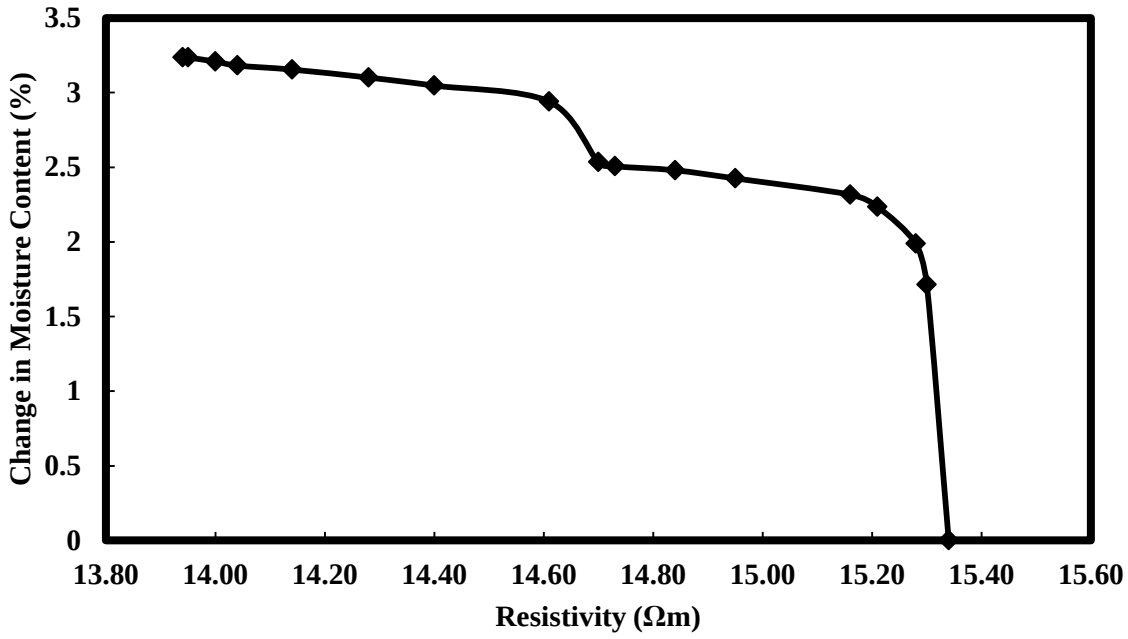

Figure – 4.20 (a) Variations in Moisture Content with Electrical Resistivity (For specimen immersed in tap water)

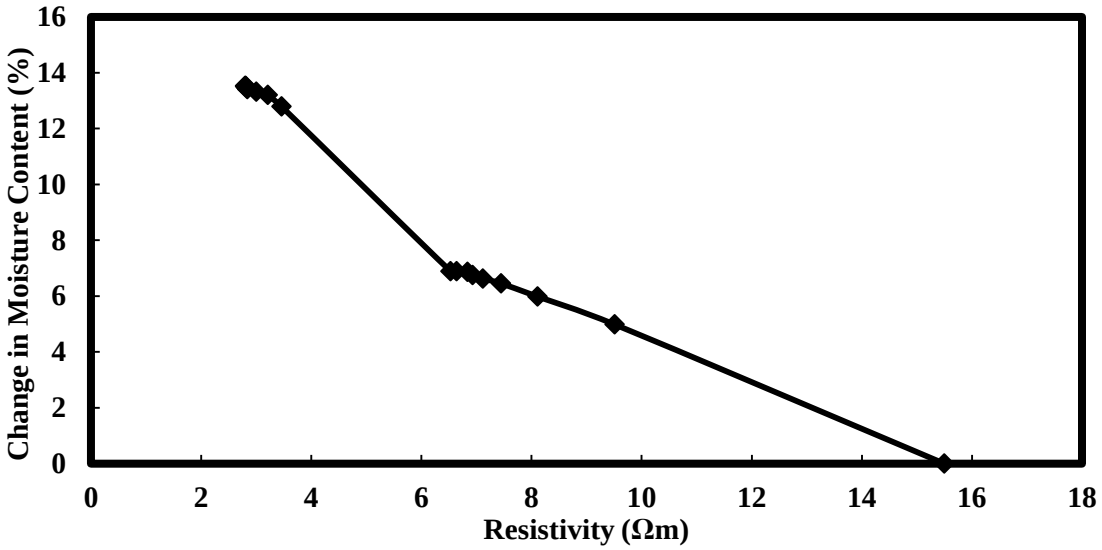

Figure – 4.20 (b) Variations in Moisture Content with Electrical Resistivity (For specimen immersed in salt water)

4.7 Summary

1. Addition of additives affects the initial resistivity, minimum resistivity, time required to reach minimum resistivity and the resistivity development through its hydration period.
2. Salt contamination decreases the initial resistivity by 97%, minimum resistivity by 93% whereas Biosurfactant contamination increases the initial resistivity by 22% and minimum resistivity by 16% as compared to Smart Cement prepared with tap water.
3. As compared to Smart Cement with tap water, 1 day resistivity decreases by 221% and 28 day resistivity by 562% due to salt contamination; whereas biosurfactant addition increased 1 day resistivity by 23% and 28 day resistivity by 120%.
4. Salt accelerates the setting time of cement whereas biosurfactant retards the setting time of cement.
5. Piezoresistive properties and the compressive strength of the specimen are also modified due to additive modification.
6. Salt contamination increases the short term (1 day) compressive strength by 45% while Biosurfactant addition decreases the short term (1 day) compressive strength by 14%

7. Long term compressive strength of smart cement specimen with UH-BS decreases by 5% is as compared to smart cement with tap water. This shows that, UH-BS could be used as a Water Reducing Admixture (WRA).
8. Short term (1 day) piezoresistive sensitivity decreases by 23% and 27% whereas long term (28 days) piezoresistive sensitivity decreases by 111% and 85% due to salt and biosurfactant contamination respectively.
9. Both, the Resistivity model and AI model predict the curing behavior very well. Though the AI model was not as effective as the resistivity model for short term curing.
10. AI model and Piezoresistivity model both were effective to predict the smart cement piezoresistive behavior for laboratory made samples.
11. Moisture detection is an advantageous and beneficial application of Smart Cement.
12. Resistivity decreased by 5% and 57% in 4 hours, upon the first contact with tap water and sea water respectively.
13. Also, moisture penetration can be differentiated between tap water and sea water on the basis of electrical resistivity values.

CHAPTER 5 WOOD

5.1 Introduction

Assessing the quality of wood has become an important procedure in forest operations, as forestry and wood processing industries are under increasing economic pressure to maximize extracted value (Wang et al. 2007a). For this reason, the estimation of timber species, quantity, and quality is critical for quantifying the productive value of a forest (Marziliano et al. 2012, Proto et al. 2014). The worldwide shift in the wood supply from old-growth forests resources to intensively managed plantations increases the need of evaluating tree quality prior to harvest (Wang & Ross 2008). The overall objective of this study was to experimentally verify the applicability of electrical method to monitor the moisture changes in wood.

5.2 Forest Distribution

The importance of forests and green lands in the development of human race needs no evidence; due to their ecological, social and economic benefits. About 33.9% of total land area of United States is forest land. However, the distribution of tree cover varies across all the states in United States. The purpose of this study is to provide an overview on the current status of America's forests.

Some historians say that when Europeans first came to America, the forests were so dense and lush that a squirrel could have travelled from Atlantic coast to Mississippi without ever touching the ground. But since then these once-lush forests have thinned out due to various natural calamities and man-made activities (Yin 2007). Besides providing aesthetic view, forests provide a range of essential benefits such as improved air and water quality, diverse wildlife habitat, prevents soil erosion and aid noise pollution. The importance of forests extends well beyond the cities and towns where they are located (Yin 2007). As per the statistics of Food and Agricultural Organization, in a period of last ten years, percent of land area covered with forests

had increased from 33.2% to 33.93%. However, there's also a formidable trend in deforestation such that United States has experienced a tree cover loss of about 8 million hectares in last ten years (Seymor 2018).

The care and management of these forests are complicated due to natural and social factors such as: wildfires, natural catastrophic events, climate change, lack of adequate management etc. As urbanization continues, these challenges are likely to increase, and new ones might emerge (Nowak 2010). Researchers are now focused on new metric named "forest attrition distance"; this reflects on removal of isolated forest patches. When these patches are lost, adjacent forest become farther apart, potentially affecting bio-diversity, local climate and many other ecological conditions. Between 1992 and 2001, the average distance between forests increased by about one-third of a mile (Yang and Mountrakis 2017).

Data regarding tree cover area of all the states in United States was collected since 2011 till 2018. States having the biggest gain and biggest losses in tree cover were then analyzed on percentage basis with respect to the total land area of respective state.

Tree cover loss in United States

Tree cover is defined as all vegetation taller than 5 meters in height as of 2000. From 2001 to 2019, United States lost 40.3Mha of relative tree cover, 10% of the global total. Brazil suffered the maximum tree cover loss of 56.5 Mha followed by 42.9 Mha tree cover loss in Canada.

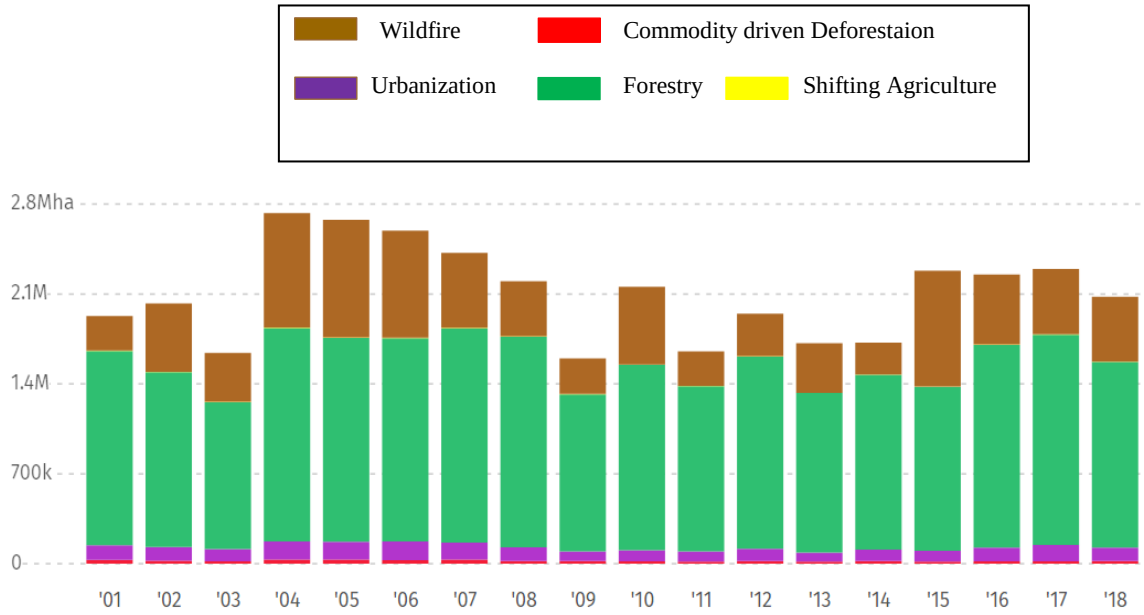

Figure – 5.1 Annual tree cover loss by dominant driver in United States

Source: Global Forest Watch

Figure – 5.1 shows the area of tree cover loss associated with the dominant driver from 2001-2018.

The five drivers are defined as follows:

1. Wildfires: Temporary loss, does not include fire clearing for agriculture.
2. Urbanization: Deforestation for expansion of urban centers.
3. Commodity driven deforestation: Large-scale deforestation linked primarily to commercial agricultural expansion
4. Forestry: Temporary loss from plantation and natural forest harvesting, with some deforestation of primary forests.
5. Shifting agriculture: Temporary loss or permanent deforestation due to small- and medium-scale agriculture

The commodity-driven deforestation and urbanization categories represent permanent deforestation, while tree cover affected by the other categories often regrows.

As per the statistics provided by Global Forest Watch (GFW), tree cover since 2011 has increased in 41 states with most increment being observed in states of Florida and Mississippi of about 4.06% and 3.41% respectively. However, biggest losses were observed in state of Texas and Wyoming by about 4.34% and 3.7% respectively. All these losses can be attributed to the factors including urbanization, natural ageing and other natural calamities. For instance; Hurricane Katrina knocked out about one third of tree shade in New Orleans whereas nearly a thousand trees were killed due to insect damage in Detroit – a city located in the Midwestern part of Michigan.

Based on the study, we can say that tree cover preservation is a major concern since; most of the current forest cover is a result of reforestation instead of preserving the old forests.

Figure 5.1 (b) represent the changes in the forest area across all the states in United States from 2016 to 2019. Figure 5.1 (c) represent the percent change in forest area over this period. Percent change has been calculated with respect to state area. From the following figures it can be seen that, Alaska and Missouri had the highest increase in forest cover of about 0.14% whereas New York had the highest decrease in forest cover of about 0.6% from 2016 to 2019.

Following plots have been plotted based on the data collected according to the statistics reported by the Forest Inventory and Analysis (FIA) Program of the U.S. Department of Agriculture Forest Service.

Following plots have been plotted based on the data collected according to the statistics reported by the Forest Inventory and Analysis (FIA) Program of the U.S. Department of Agriculture Forest Service.

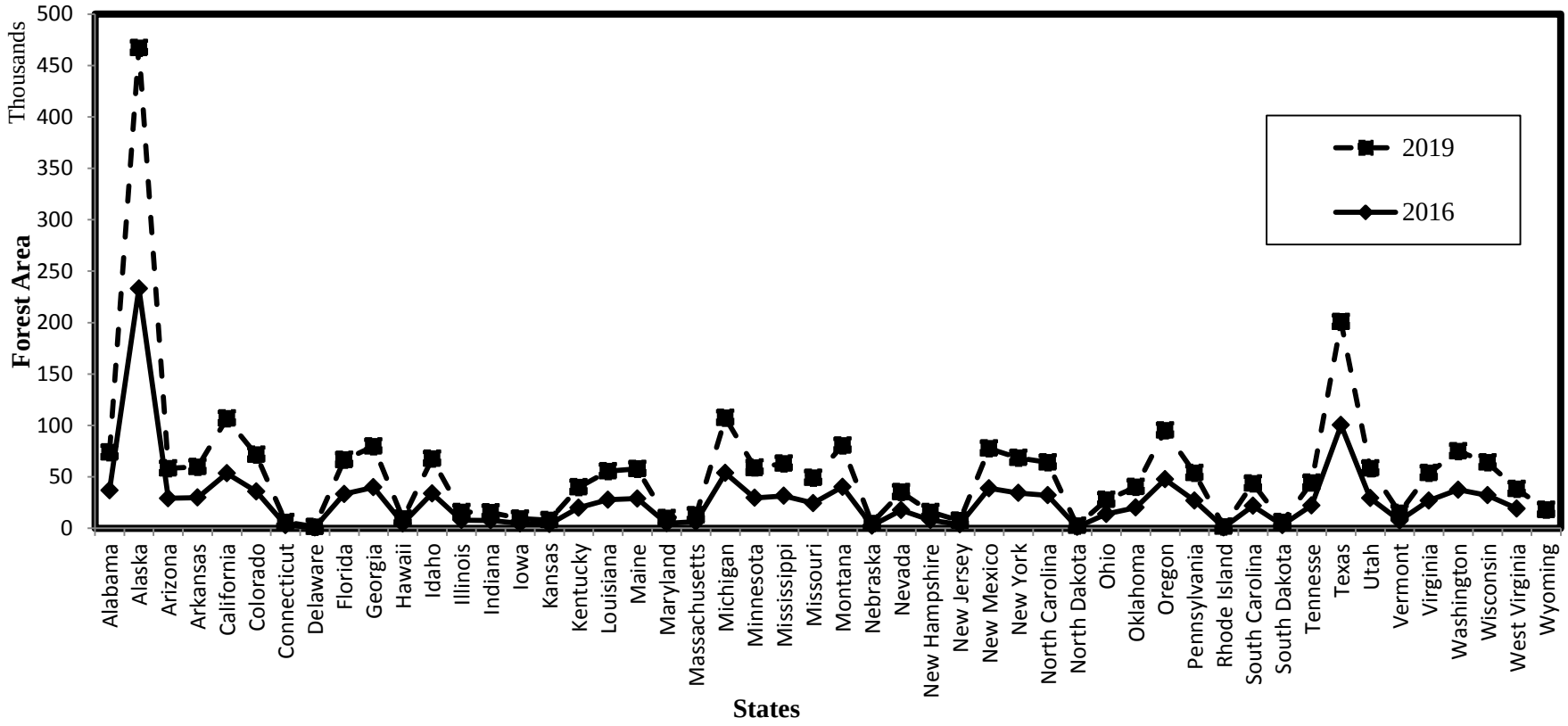

Figure – 5.1(b) Change in Forest Area across US

Source: Forest Inventory Analysis

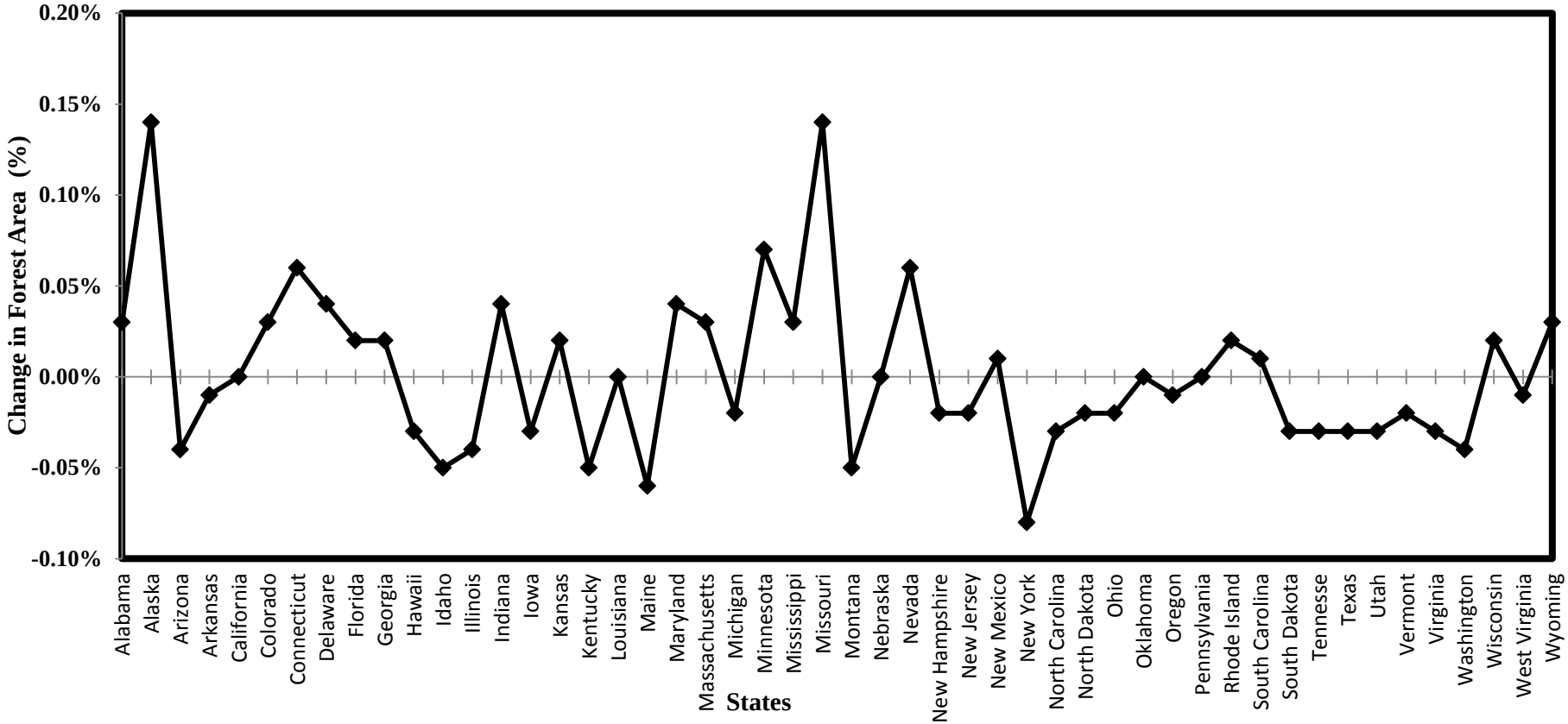

Figure – 5.1(c) Percent change in forest area across US

Source: Forest Inventory Analysis

5.3 Impedance vs Frequency

Using an LCR, R and X were noted for different combinations and Electrical Impedance was calculated. Electrical Impedance is calculated using the following equation:

$$Z = [(R^2 + X^2)^{1/2}] \qquad (5.1)$$

Here, R and X are noted from an LCR at different frequencies.

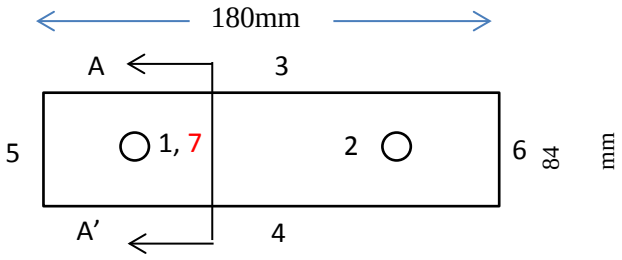

Plan View

Figure – 5.2 Plan view of the wooden specimen with connections

Points 1 – 7 are the points located on the sample to measure the Resistance values in different directions. Points 1 and 2 are on the same face of the sample parallel to the direction of fibers whereas 1 and 7 are on the opposite of sample. LCR meter was used to measure the Resistance of the wooden sample. Wood was tested for different connection:

5.3.1 Clamped Connection: Contacts (wires) were clamped to the specimen

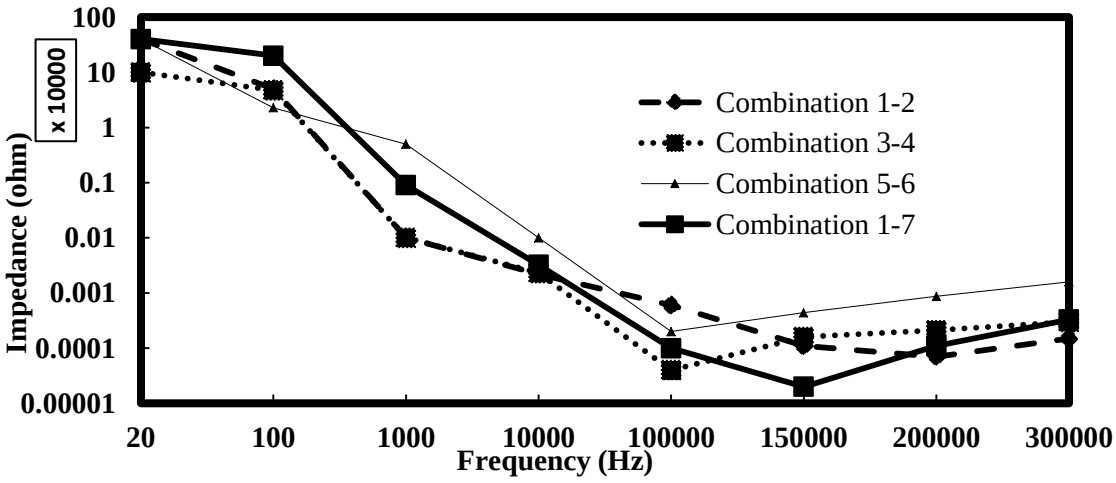

Figure – 5.3 Variation of Impedance with frequency for clamped connection

5.3.2 Screwed Connection: Screws were used as contacts.

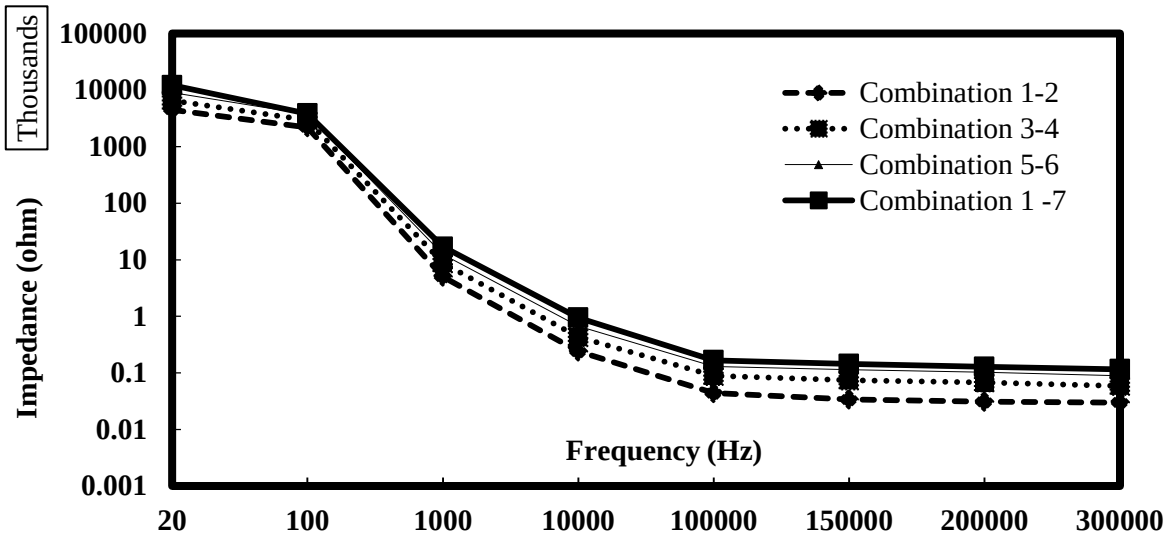

Figure – 5.4(a) Variation of Impedance with frequency for screwed connection

Visual analysis during experiments indicated that Resistance values for screwed connection were stable than those for clamped connection. Hence, screwed connection was adopted for this study.

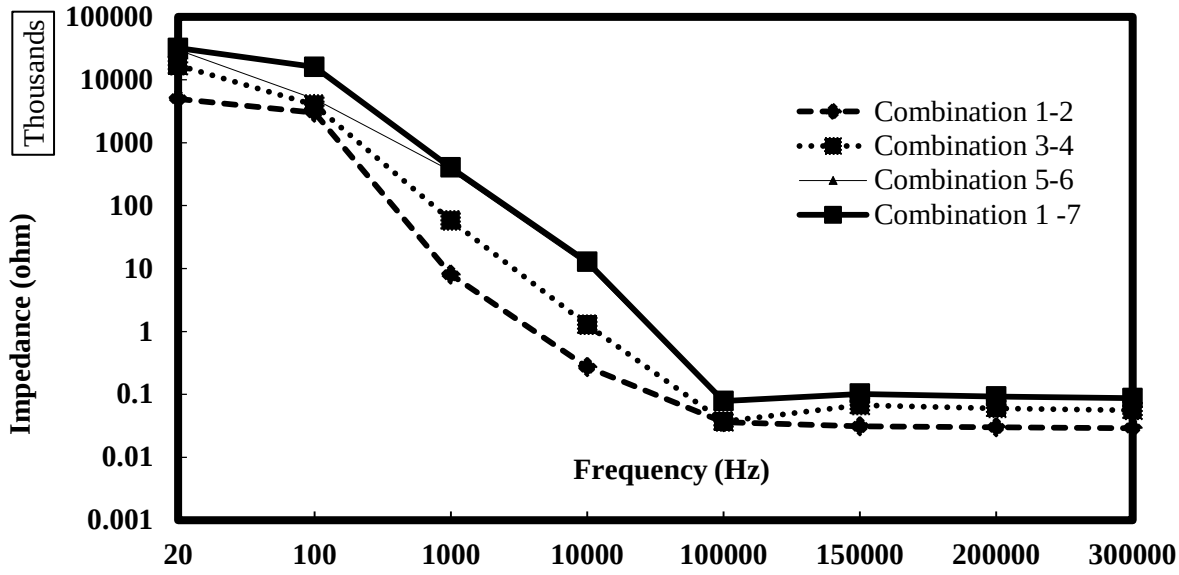

Figure – 5.4 (b) Variation of Impedance with frequency for screwed connection

Figure 5.4 (b) represents the variation of impedance with frequency for screwed connection. The similarity in the impedance trends for screwed connection can be observed (Figure – 5.4 (a) and (b)).

5.4 Moisture Variations

Figure – 5.5 represents the changes in weight of wood specimen when exposed to different conditions. Initially, weight of the wood was measured in unsaturated condition and then oven dried (30 minutes @45^{o}C). Wood specimens were then submerged in tap water and salty water for a period of 24 hours; electrical properties and weight of the specimen were recorded.

Weight of the specimen in unsaturated condition was 288.9 grams which reduced by 0.2% after oven drying. Weight of the specimen increased by 8%, 11% 13% and 14% on immersing the specimen in tap water for 1, 6, 12 and 24 hours respectively (Figure 5.5). Similar test was conducted for another specimen immersed in salty water (Salinity 35gm/L). Weight of the specimen increased by 11%, 13% 14% and 16% on immersing the specimen in salty water for 1, 6, 12 and 24 hours respectively (Figure – 5.5).

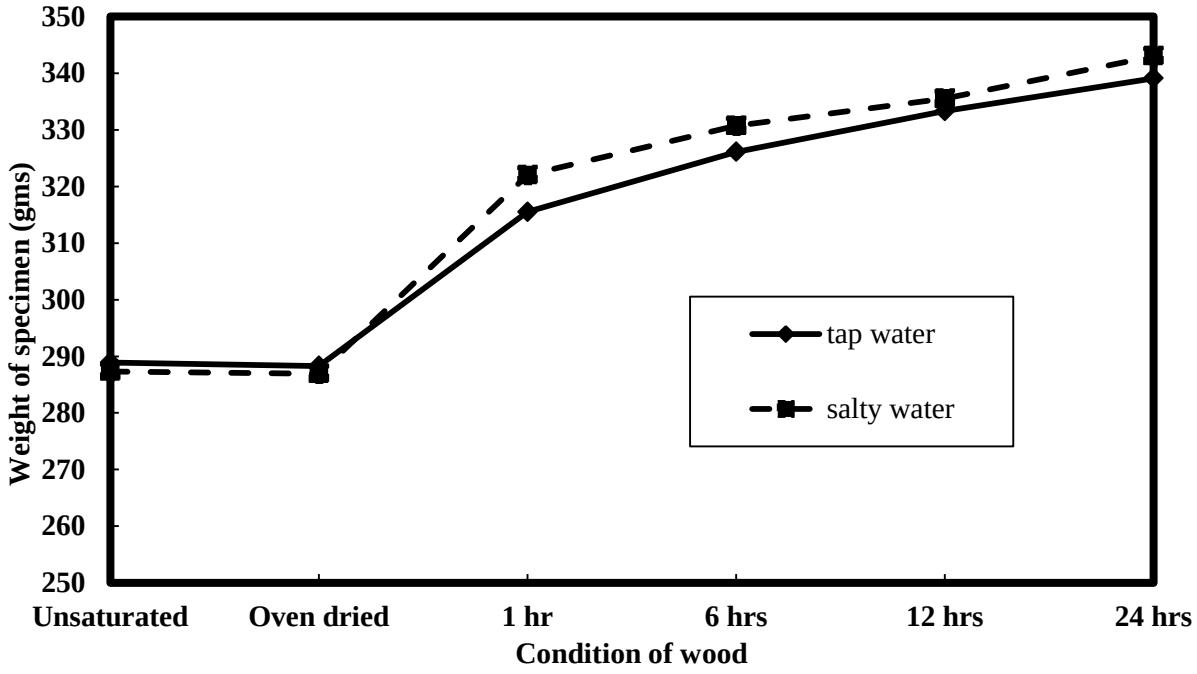

Figure – 5.5 Variations in weight of wood immersed in tap water and salty water.

Electrical Resistance was noted for the wooden specimen in different conditions at different frequencies. Table – 5.1 (a) to (d) represent the directional resistance and change in resistance (ΔR/Ro) of wood for different conditions. It can be seen that on immersion of wood in water, electrical resistance of the specimen decreases. This could be due to the reason that water gets into the specimen and fills the air voids and as resistance of water is less than that of air, resistance decreases. Also, electrical resistance goes negative from 150 kHz and the change in resistance (ΔR/Ro) values are positive only for 100 kHz. Hence, 100 kHz can be used for measurements of electrical properties of wood.

Table – 5.1(a) Variation in Resistance of wood for combination 1-2 in different conditions

COMBINATION 1-2											
FREQUENCY	**UNSATURATED**	**OVEN DRIED**	**ΔR/Ro**	**1hr**	**ΔR/Ro**	**6hrs**	**ΔR/Ro**	**12hrs**	**ΔR/Ro**	**24hrs**	**ΔR/Ro**
	(A)	**(B)**	((B-A)/A)*100	(C)	((C-A)/A)*100	(D)	((D-A)/A)*100	(E)	((E-A)/A)*100	(F)	((F-A)/A)*100
	(Ro)		**(%)**		**(%)**		**(%)**		**(%)**		**(%)**
20	5000000000	4000000000	-25.00	400000	-99.99	85000	99.99	100000	-99.99	81000	-99.99
100	3000000000	980000000	-206.12	440000	-99.98	369000	-99.98	155000	-99.99	147200	-2037943.48
1000	8000000	5000000	-60.00	278000	-2777.70	224000	-3471.43	120000	-6566.67	115000	-6856.52
10000	270000	100000	-170.00	234000	-15.38	175000	-54.29	98000	-175.51	89200	-202.69
100000	5000	7000	28.57	204000	97.55	120000	95.83	970000	99.48	85000	94.12
150000	-17000	-1000	-1600.00	195000	108.72	97000	117.53	81000	120.99	77000	122.08
200000	-44000	-21000	-109.52	160000	127.50	77000	157.14	60000	173.33	53000	183.02
300000	-64000	-36000	-77.78	169000	137.87	1100000	105.82	77000	183.12	66000	196.97

Table – 5.1(b) Variation in Resistance of wood for combination 3-4 in different conditions

COMBINATION 3-4											
FREQUENCY	**UNSATURATED**	**OVEN DRIED**	**ΔR/Ro**	**1hr**	**ΔR/Ro**	**6hrs**	**ΔR/Ro**	**12hrs**	**ΔR/Ro**	**24hrs**	**ΔR/Ro**
	(A)	**(B)**	((B-A)/A)*100	(C)	((C-A)/A)*100	(D)	((D-A)/A)*100	(E)	((E-A)/A)*100	(F)	((F-A)/A)*100
	(Ro)		**(%)**		**(%)**		**(%)**		**(%)**		**(%)**
20	12000000000	8800000000	-36.36	469000	-2558535.39	254000	-4724309.45	87000	-13793003.45	79000	$-15189x10^{3}$
100	1000000000	1000000000	0	333000	-570	200000	-1.89×10^{10}	73000	-2601	72000	#-2637
1000	50000000	6000000	-733.33	254000	-19585.04	178000	-27989.89	110000	-45354.55	80000	-62400.00
10000	1000000	104000	-861.54	190000	-426.32	160000	-525.00	35000	-2757.14	30000	-3233.33
100000	1000	3000	66.67	178000	99.44	135000	99.26	31000	96.77	29750	96.64
150000	36000	-4500	900.00	104000	65.38	85000	57.65	30000	-20.00	29750	-21.01
200000	-121000	-11000	-1000.00	47000	357.45	46000	363.04	29000	517.24	25400	576.38
300000	-200000	-50000	-300.00	81000	346.91	78000	356.41	44000	554.55	25400	887.40

Table – 5.1(c) Variation in Resistance of wood for combination 5-6 in different conditions

COMBINATION 5-6											
FREQUENCY	**UNSATURATED**	**OVEN DRIED**	**ΔR/Ro**	**1hr**	**ΔR/Ro**	**6hrs**	**ΔR/Ro**	**12hrs**	**ΔR/Ro**	**24hrs**	**ΔR/Ro**
	(A)	**(B)**	((B-A)/A)*100	(C)	((C-A)/A)*100	(D)	((D-A)/A)*100	(E)	((E-A)/A)*100	(F)	((F-A)/A)*100
	(Ro)		**(%)**		**(%)**		**(%)**		**(%)**		**(%)**
20	13000000000	5000000000	-160.00	365000	-3561543.84	263000	-4942865.78	137000	-9488951.09	144000	-9027677.78
100	1000000000	1000000000	0.00	320000	-312400.00	196000	-510104.08	136000	-735194.12	125100	-799260.51
1000	300000000	2000000	-14900.00	299000	-100234.45	146000	-205379.45	98000	-306022.45	84000	-357042.86
10000	10000000	43000	-23155.81	265000	-3673.58	133500	-7390.64	72100	-13769.63	91000	-10889.01
100000	260000	11000	-2263.64	247000	-5.26	120000	-116.67	100000	-160.00	87000	-198.85
150000	67000	-1100	6190.91	227000	70.48	114000	41.23	960000	93.02	81100	17.39
200000	-11000	-74000	85.14	190000	105.79	83000	113.25	820000	101.34	61000	118.03
300000	720000	-100000	820.00	269000	-167.66	1250000	42.40	120000	-500.00	63000	-1042.86

Table – 5.1(d) Variation in Resistance of wood for combination 1-7 in different conditions

COMBINATION 1-7											
FREQUENCY	**UNSATURATED**	**OVEN DRIED**	**ΔR/Ro**	**1hr**	**ΔR/Ro**	**6hrs**	**ΔR/Ro**	**12hrs**	**ΔR/Ro**	**24hrs**	**ΔR/Ro**
	(A)	**(B)**	((B-A)/A)*100	(C)	((C-A)/A)*100	(D)	((D-A)/A)*100	(E)	((E-A)/A)*100	(F)	((F-A)/A)*100
	(Ro)		**(%)**		**(%)**		**(%)**		**(%)**		**(%)**
20	2000000000	8000000000	75.00	781000	-255981.95	232500	-860115.05	77000	-2597302.60	740000	-270170.27
100	11000000000	2000000000	-450.00	560000	-1964185.71	199000	-5527538.19	173000	-6358281.50	152000	-7236742.11
1000	44000000	710000000	93.80	325000	-13438.46	169250	-25897.05	100000	-43900.00	99000	-44344.44
10000	1500000	78000	-1823.08	191000	-685.34	156000	-861.54	87000	-1624.14	84000	-1685.71
100000	45000	6750	-566.67	185000	75.68	120000	62.50	56000	19.64	51000	11.76
150000	6000	120	-4900.00	179000	96.65	96000	93.75	50000	88.00	47000	87.23
200000	-12000	-9000	-33.33	165000	107.27	87000	113.79	43000	127.91	39000	130.77
300000	-58000	-11500	-404.35	175000	133.14	1000000	105.80	58000	200.00	51000	213.73

From Table – 5.1 (a) – (d), it can be seen that ΔR/Ro is positive for frequency of 100 kHz. But there is a variation in the data for combination 5 – 6 (Table – 5.1 (c)), as the ΔR/Ro values are negative. This could be explained due to a cracking in the wood. (Figure – 5.6).

Figure – 5.6 Cracking in wood

5.5 Ultrasonice Pulse Velocity

Figure 5.7 represents the changes in the Ultrasonic Pulse Velocity of the specimens with changes in moisture content. Initially the specimen was oven dried for 30 minutes at @45^{o}C. It was then immersed in tap water for upto 24 hours and UPV was recorded. Similar test was conducted on specimen immersed in salty water (salinity 35 gm/L). It can be seen that, on oven-drying the specimen; the UPV increases as compared to that of in unsaturated condition. Further, on immersing the specimen in tap water for upto 24 hours, UPV decreases gradually. This could be because on drying the specimen, water evaporates and the voids are filled with air. As the Ultrasonic Pulse Velocity of air is more than that of water, Ultrasonic Pulse Velocity of the specimen increases on drying and decreases on immersion in water. Similar trend was also observed for specimen-2 immersed in salty water.

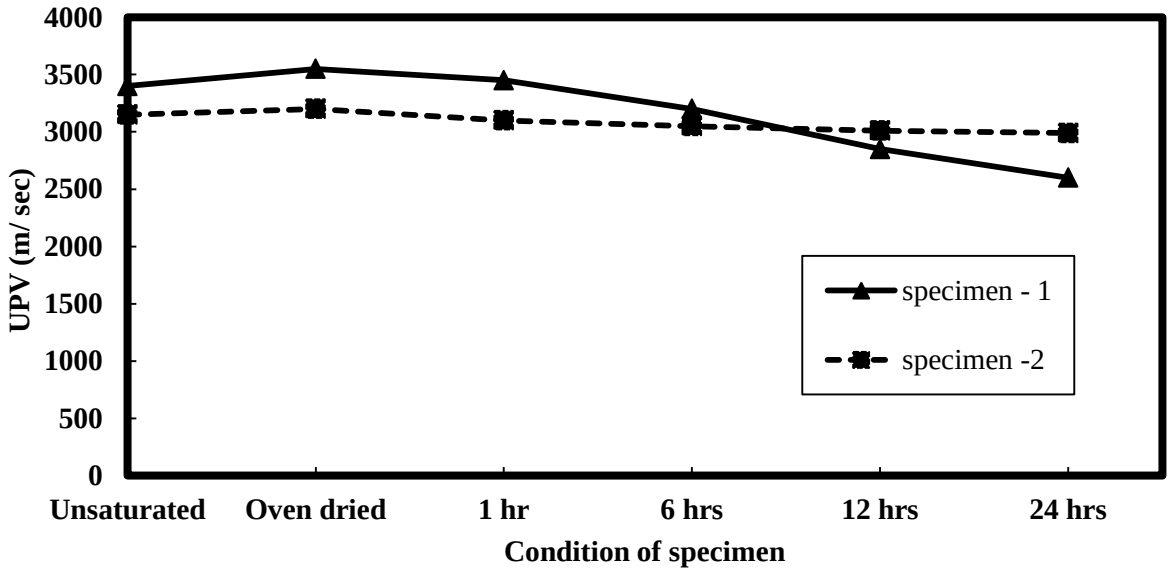

Figure – 5.7 Variation in UPV with moisture changes

On immersing the specimen for 24 hours in tap water, UPV decreased by 36% whereas on immersing the specimen in salty water, it decreased by about 7%. This shows that salt penetrates in the specimen and plugs the air voids and affects the wave speed.

5.6 Summary

1. Based on the study, we can say that tree cover preservation is a major concern since; most of the current forest cover is a result of reforestation instead of preserving the old forests.
2. As screwed connection offer better stability of results, screwed connection was adopted for this study.
3. 100 kHz can be used as a frequency for measurements of wood.
4. Ultrasonic Pulse Velocity could be used as a measurement technique for moisture detection. Also, moisture penetration can be differentiated based on the changes in Ultrasonic Pulse Velocity of the specimen.

CHAPTER 6 CONCLUSIONS AND RECOMMENDATIONS

6.1 Conclusions

Based on this study, following conclusions can be advanced:

1. Smart Cement, chemo-piezo sensitive cement is a suitable material for real time monitoring through the service life of the structure, with electrical resistivity as a sensing parameter magnifying changes upto 2000 times.
2. Salt contamination decreases the initial resistivity by 97%, minimum resistivity by 93% whereas Biosurfactant contamination increases the initial resistivity by 22% and minimum resistivity by 16% as compared to Smart Cement prepared with tap water.
3. As compared to Smart Cement with tap water, 28 day resistivity decreased by 562% due to salt contamination; whereas biosurfactant addition increased 28 day resistivity by 120%.
4. Salt contamination increases the short term (1 day) compressive strength by 45% while Biosurfactant addition decreases the short term (1 day) compressive strength by 14%
5. Long term compressive strength of smart cement specimen with UH-BS decreases by 5% as compared to smart cement with tap water. This shows that, UH-BS could be used as a Water Reducing Admixture (WRA).
6. Long term (28 days) piezoresistive sensitivity decreased by 111% and 85% due to salt and biosurfactant contamination respectively.
7. Moisture detection is an advantageous and beneficial application of Smart Cement. Also, moisture penetration can be differentiated between salted and unsalted water on the basis of change in electrical resistivity values.
8. Tree cover preservation is a major concern since; most of the current forest cover is a result of reforestation instead of preserving the old forests.
9. 100 kHz should be used as a frequency for measurements of wood.

10. Ultrasonic Pulse Velocity (UPV) decreased by about 36% and 7% on about 15% moisture infiltration of nonsaline and saline water respectively. Change in the UPV can be used as a correlation to determine the moisture changes in wood.

6.2 Recommendations

Based on the results of this study, following suggestions are offered for future studies:

1. LCR device was used to monitor the changes in the electrical properties of the cementitious composites. New instruments can be developed, to prove the effectiveness of electrical characterization in different fields.
2. Use of other additional additives can be initiated to improve the sensitivity of smart cement with contaminations.
3. Novel measurement technique or data acquisition system can be developed to determine the resistivity of wood.
4. Real time monitoring along with the implementation of Artificial Intelligence can help to better predict the stresses in the cementitious materials.

REFERENCES

Akankpo, O., & MU, I. (2011). “Monitoring groundwater contamination using surface electrical resistivity and geochemical methods.” *Journal of Water Resource and Protection*, 2011.

Azhari, F. and Banthia, N. (2012). “Cement-based sensors with carbon fibers and carbon nanotubes for piezoresistive sensing, cement and concrete composites.” Vol. 34, pp. 866–873.

Bastos, G., Patiño-Barbeito, F., Patiño-Cambeiro, F., & Armesto, J. (2016). “Admixtures in cement-matrix composites for mechanical reinforcement, sustainability, and smart features.” *Materials*, 9(12), 972.

Bhatia, S., Vipulanandan, C. (2020). Effect of Salt contamination on the long term Compressive Strength and Piezoresistive sensitivity of Smart Cement. CIGMAT-2020 Conference & Exhibition – Proceedings, II-24-II-27.

Bhatia, S., Vipulanandan, C. (2020). Effect of UH-Biosurfactant on the performance of Smart Cement. CIGMAT-2020 Conference & Exhibition – Proceedings, II-20-II-23.

Brandt, A. (2009) Cement-Based Composites: Materials, Mechanical Properties and Performance, 2nd ed.; CRC Press: Boca Raton, FL, USA.

Brashaw, B. K., Wang, X., Ross, R. J., & Pellerin, R. F. (2004). “Relationship between stress wave velocities of green and dry veneer.” *Forest products journal*. Vol. 54, no. 6 (June 2004): Pages 85-89.

Calegari, L., Gatto, D. A., & Stangerlin, D. M. (2011). “Influence of moisture content, specific gravity and specimen geometry on the ultrasonic pulse velocity in Eucalyptus grandis Hill ex Maiden wood.” Revista Ciência da Madeira (Brazilian Journal of Wood Science), 2(2), 10-12953.

Coppola, L., Buoso, A., & Corazza, F. (2013). “The influence of AC and DC electrical

resistance and piezoresistivity measurements of CNTs/cement composites." *The New Boundaries of Structural Concrete Session B.*

Dormehl, L. (2019). What is an artificial neural network? Here's everything you need to know. Emerging Tech.

Hambach, M., Möller, H., Neumann, T., & Volkmer, D. (2016). "Carbon fibre reinforced cement-based composites as smart floor heating materials." Composites Part B: Engineering, 90, 465-470.

Han, B. G., Han, B. Z., & Ou, J. P. (2009). "Experimental study on use of nickel powder-filled Portland cement-based composite for fabrication of piezoresistive sensors with high sensitivity." *Sensors and Actuators A: Physical*, 149(1), 51-55.

Han, B., Yu, X., & Kwon, E. (2009). "A self-sensing carbon nanotube/cement composite for traffic monitoring." *Nanotechnology*, 20(44), 445501.

Hasenstab, A., Osterloh, K., & Krause, M. (2006, September). Testing of wooden construction elements with ultrasonic echo technique and X-ray. In Proceedings of the 9th European Conference on Non-Destructive Testing, Berlin, Germany (pp. 25-29).

Hewlett, P. (2004). Lea's Chemistry of Cement and Concrete, 4th edition; Butterworth-Heinemann: Oxford, UK.

Husein, I., Agustina, A., & Khabibi, J. (2014). "Electrical properties of Indonesian hardwood case study: Acacia mangium, Swietenia macrophylla and Maesopsis eminii." *Wood research* 59 (4): 695-704

Kramer, J.T. (2006). "The Importance of Wood." *International Woodworking magazine*

Kumar, M., & Gupta, R. C. (1993). "Electrical resistivity of Acacia and Eucalyptus wood chars." *Journal of materials science*, 28(2), 440-444.

Li, W., Li, X., Chen, S. J., Liu, Y. M., Duan, W. H., & Shah, S. P. (2017). "Effects of graphene oxide on early-age hydration and electrical resistivity of Portland cement paste." *Construction and Building Materials*, 136, 506-514.

Li, Z., Wei, X., & Li, W. (2003). “Preliminary interpretation of Portland cement hydration process using resistivity measurements.” *Materials Journal*, 100(3), 253-257.

Liao, Y., & Wei, X. (2014). “Relationship between chemical shrinkage and electrical resistivity for cement pastes at early age.” *Journal of materials in civil engineering*, 26(2), 384-387.

Liao, Y., & Wei, X. (2014). “Relationship between chemical shrinkage and electrical resistivity for cement pastes at early age.” *Journal of materials in civil engineering*, 26(2), 384-387.

Marziliano, P. A., Menguzzato, G., Scuderi, A., & Corona, P. (2012). Simplified methods to inventory the current annual increment of forest standing volume. iForest-Biogeosciences and Forestry, 5(6), 276.

Mulligan, C. N. (2005). Environmental applications for biosurfactants. Environmental pollution, 133(2), 183-198.

Nowak, D. J., Randler, P. B., Greenfield, E. J., Comas, S. J., Carr, M. A., & Alig, R. J. (2010). Sustaining America's urban trees and forests: A Forests on the Edge report. US Department of Agriculture, Forest Service, Northern Research Station. NRS- 62.

Panda, Guru (2020). “Real-Time Monitoring and Characterization of Smart Cement and Soil with Polymer Modification to Control Gas Leakage and Corrosion.” University of Houston, Houston, Texas

Piccinini, G. (2004). The First computational theory of mind and brain: a close look at mcculloch and pitts's “logical calculus of ideas immanent in nervous activity”. Synthese, 141(2), 175-215.

Pimenta Teixeira, K., Perdigão Rocha, I., De Sá Carneiro, L., Flores, J., Dauer, E. A., & Ghahremaninezhad, A. (2016). “The effect of curing temperature on the properties of cement pastes modified with TiO2 nanoparticles”. *Materials*, 9(11), 952.

Proto, A. R., Macrì, G., Bernardini, V., Russo, D., & Zimbalatti, G. (2017). “Acoustic

evaluation of wood quality with a non-destructive method in standing trees: a first survey in Italy." iForest-Biogeosciences and Forestry, 10(4), 700.

Sahin, H., & Ay, N. (2004). "Dielectric properties of hardwood species at microwave frequencies." *Journal of Wood Science*, 50(4), 375-380.

Saleh, F. K., Rivera, R., Salehi, S., Teodoriu, C., & Ghalambor, A. (2018, February). "How does mixing water quality affect cement properties." SPE International Conference and Exhibition on Formation Damage Control. Society of Petroleum Engineers.

Sanesi G, Lafortezza R, Colangelo G, Marziliano PA, Davies C (2013). Root system investigation in sclerophyllous vetgetation: an overview. *Italian Journal of Agronomy* 8: 121-126.

Seymour, F. (2018). Deforestation is accelerating, despite mounting efforts to protect tropical forests. what are we doing wrong?. Blog of Global Forest Watch, June, 27, 2018.

Shi, L., Lu, Y., & Bai, Y. (2017). "Mechanical and electrical characterization of steel fiber and carbon black engineered cementitious composites." Procedia Engineering, 188, 325-332.

Spragg, R., Villani, C., Snyder, K., Bentz, D., Bullard, J. W., & Weiss, J. (2013). "Factors that influence electrical resistivity measurements in cementitious systems." Transportation Research Record, 2342(1), 90-98.

Stamm, A. J. (1927). "The Electrical Resistance of Wood as A Measure of Its Moisture Content." Industrial & Engineering Chemistry, 19(9), 1021-1025.

Sun, M. Q., Li, J., Wang, Y. J., & Zhang, X. Y. (2015). "Preparation of carbon fiber reinforced cement-based composites using self-made carbon fiber mat." *Construction and Building Materials*, 79, 283-289.

Thomas, K., & Lisk, W. E. A. (1970). "Effect of sea water from tropical areas on setting times of cements." *Matériaux et constructions*, 3(2), 101-105.

Vipulanandan, C. and Garas, V. (2008). "Electrical resistivity, pulse velocity and

compressive properties of carbon fiber reinforced cement mortar." *Journal of Materials in Civil Engineering*, Vol. 20, pp. 93-101.

Vipulanandan, C. and Prashanth, P. (2013). "Impedance spectroscopy characterization of a piezoresistive structural polymer composite bulk sensor." *Journal of Testing and Evaluation*, Vol. 41, pp. 898-904.

Vipulanandan, C., and Garas, V. (2006), "Piezoresistivity of Carbon Fiber Reinforced Cement Mortar." Proceedings, Engineering, Construction and Operations in Challenging Environments, Earth & Space 2006, Proceedings ASCE Aerospace Division, League City, TX, CD-ROM.

Vipulanandan, C., and Sett, K. (2004). "Development and Characterization of Piezoresistive Smart Structural Materials," Proceedings, Engineering, Construction and Operations in Challenging Environments, Earth & Space 2004, ASCE Aerospace Division, League City, TX, pp. 656-663.

Vipulanandan, C., Ganapathy, C., Gebreselassie, K. A., Pan, D., Panda, G., & Ganpatye, A. S. (2019, April). "New Rapid Nondestructive Testing Method for Detecting and Quantifying with Material Property Changes Using Vipulanandan Impedance Corrosion Model." In *Offshore Technology Conference*. Offshore Technology Conference.

Vipulanandan, C., Aldughather, A., Panda, G., & Wong, G. (2020, January). Real-Time Gas Leak Detection and Quantification using Smart Cement. In *International Petroleum Technology Conference*. International Petroleum Technology Conference.

Wang, X., Carter, P., Ross, R. J., & Brashaw, B. K. (2007). "Acoustic assessment of wood quality of raw forest materials: a path to increased profitability." *Forest products journal.* Vol. 57, no. 5 (May 2007): Pages 6-14.

Wang, X., Ross, R. J., & Carter, P. (2007). "Acoustic evaluation of wood quality in standing trees. Part I. Acoustic wave behavior." *Wood and Fiber Science,* 39(1), 28-38.

Yang, S., & Mountrakis, G. (2017). Forest dynamics in the US indicate disproportionate

attrition in western forests, rural areas and public lands. PloS one, 12(2),

Yin, S. (2017) How far to the next forest? A new way to measure deforestation. The New York Times.

Youngs , R. History, Nature and Products of Wood. Forests and Forest Plants, Vol II.

Yue, X., Wang, L., Shi, X., Xu, M., & Zhu, Z. (2018). “Investigations on the effects of seasonal temperature changes on the electrical resistance of living trees.” *Forests*, 9(9), 550.

Yue, X., Wang, L., Wacker, J. P., & Zhu, Z. (2019). “Electric resistance tomography and stress wave tomography for decay detection in trees—a comparison study.” *PeerJ*, 7, 6444.

Zhang, C., Yan, Q., Panda, G. P., Wu, W., Song, G., & Vipulanandan, C. (2020). “Real-time monitoring stiffness degradation of hardened cement paste under uniaxial compression loading through piezoceramic-based electromechanical impedance method.” *Construction and Building Materials*, *256*, 119395.